Effects of scalar leptoquark on semileptonic Λ_b decays

Suchismita Sahoo and Rukmani Mohanta

School of Physics, University of Hyderabad, Hyderabad - 500046, India

arXiv:1607.04449v2 [hep-ph] 6 Sep 2016

Abstract

We study the scalar leptoquark effects on the rare semileptonic decays of Λ_b baryon, governed by the quark level transition $b \to s l^+ l^-$. We estimate the branching ratios, forward-backward asymmetries, lepton polarization parameters and the lepton flavour non-universality effects in these decay channels. We find significant deviations from the corresponding standard model predictions in some of the observables due to leptoquark effects. We also investigate the lepton flavour violating decays $\Lambda_b \to \Lambda l_i^- l_j^+$, the branching ratios of which are found to be $\mathcal{O}(10^{-10} - 10^{-9})$.

PACS numbers: 13.30.Ce, 14.80.Sv

I. INTRODUCTION

The study of the rare B meson decays involving flavour changing neutral current (FCNC) transitions is very crucial, as they provide sensitive probe to look for new physics (NP) beyond the standard model (SM). These decays are highly suppressed in the SM due to Glashow-Iliopoulos-Maiani (GIM) mechanism and occur only through one-loop level penguin and box diagrams. Recently, several anomalies have been observed in the rare semileptonic B decays mediated through the FCNC $b \to s$ transitions. The most prominent ones are the observation of 3.7σ deviation in the angular observable P_5' [1–3] of $B \to K^* \mu^+ \mu^-$ mode and the violation of lepton universality in the $B \to K l^+ l^-$ decays at the level of 2.6σ [4] by the LHCb experiment. In addition, LHCb has also observed significant discrepancy in the decay rates of the $B \to K^* l^+ l^-$ processes [5, 6]. Also the decay rate of the $B_s \to \phi \mu^+ \mu^-$ process [7] has 3.3σ deviation form its SM value in the low q^2 region. Furthermore, the observed discrepancy in the ratio of branching fractions of exclusive $B \to K^{(*)} l^+ l^-$ decay and the inclusive decays into dimuon over dielectron in the full q^2 range [8] provide strong evidence of the presence of lepton non-universality.

The anomalies observed in $b \to s l^+ l^-$ processes at LHCb [1, 2, 4–7] have attracted a lot of attention in recent times. The implications of these observations have been extensively studied both in the context of various new physics models and in model independent ways [9–13]. These deviations which are at the level of (2-3)σ are not statistically significant enough to provide an unambiguous signal of new physics. On the other hand they are also not small enough to be ignored completely and need to be scrutinized meticulously as many different ways as possible. If indeed they really evince the smoking gun signal of some kind of NP, such effects must also show up in other decay channels involving $b \to s$ transitions, such as the corresponding Λ_b transitions. Therefore, the study of the rare Λ_b decays is of utmost importance to obtain an unambiguous signal of new physics. Including the baryonic decay mode $\Lambda_b \to \Lambda(\to p\pi^-)\mu^+\mu^-$ in the Bayesian analysis of $|\Delta B| = |\Delta S| = 1$ transitions, a fit of the Wilson coefficients $C_{9,10,}$, $C'_{9,10}$ has been performed in Ref. [14], and it has been shown that, the shift to C_9 prefers to be opposite to the one found in mesonic case. To be more specific, the shift in C_9 in baryonic decay is found to be $\Delta_9 = C_9 - C_9^{SM} = 1.6^{+0.7}_{-0.9}$, as compared to the mesonic case where its value is $\Delta_9 = -1.09^{+0.22}_{-0.20}$ [11]. Whereas the corresponding shifts in C_{10} are in the same direction, i.e., $\Delta_{10} = 0.7^{+0.5}_{-0.8}$ for the baryonic

case $\Delta_{10} = 0.56^{+0.25}_{-0.24}$ for mesonic case. As pointed out in [14], the observed discrepancy in the shift of C_9 might arise from our incomplete understanding of the hadronic matrix elements of the two-point correlators of $\mathcal{O}_{1,\cdots,6;8}$ with the quark electromagnetic current, which effectively shift the Wilson coefficients C_7 and C_9. This could also be due to the large experimental uncertainties for the $\Lambda_b \to \Lambda(\to p\pi)\mu^+\mu^-$ observables. However, if this persists with improved statistics, this would constitute a breakdown of the universal structure of the transversity amplitudes at low recoil, as predicted by the operator product expansion (OPE).

The important distinction between the Λ_b baryon and B meson decays is the spin of the Λ_b baryon. Therefore, the number of degrees of freedom involved in the bound state of baryon is more, hence the systematic study of $\Lambda_b \to \Lambda\gamma$ and $\Lambda_b \to \Lambda\mu^+\mu^-$ are relatively less explored in comparison to their mesonic counter parts. Also the experimental data on various Λ_b decay channels are rather limited. Recently LHCb has reported the branching ratio of $\Lambda_b \to \Lambda\mu^+\mu^-$ [15], which is found to be lower than its standard model prediction. This decay process has been extensively studied in the literature both in the SM and in various beyond the SM scenarios [16–23]. To supplement these studies, in this paper we would like to analyze the rare baryonic decay processes $\Lambda_b \to \Lambda l^+ l^-$, where $l = e, \mu, \tau$ in the scalar leptoquark model. In recent times, the scalar leptoquark model has been received a lot of attention, as it can successfully explain most of the observed anomalies associated with the $b \to sll$ transitions. Leptoquarks are color-triplet bosonic particles which can couple to a quark and lepton pair at the same time. The existence of leptoquark has been proposed in many extensions of the SM, such as grand unification model [24, 25], Pati-Salam model [26], extended technicolor model [27] and the composite models [28]. The leptoquark states can be classified as vectors (spin-1) or scalars (spin-0). They can be characterized by their Fermion no. $F = 3B + L$, where B and L are the baryon no. and lepton no. respectively. Scalar leptoquarks may exist at TeV scale, and can give observable signatures in various low energy processes [33]. The phenomenology of scalar leptoquarks has been studied extensively in the literature [29–37]. In this paper, we would like to study the rare baryonic decay processes $\Lambda_b \to \Lambda l^+ l^-$ in the scalar leptoquark model. In particular, we estimate the decay rates, forward-backward (A_{FB}) and lepton polarization asymmetries in these modes. Furthermore, we explore the possibility of lepton non-universality parameter in Λ_b decays and also the lepton flavour violating (LFV) decays mediated via the scalar leptoquarks.

The paper is organized as follows. In Section II we present the effective Hamiltonian responsible for the $b \to s l^+ l^-$ processes and the decay parameters for the semileptonic $\Lambda_b \to \Lambda l^+ l^-$ decays in the standard model. The new physics contribution due to the exchange of scalar leptoquark has been presented in section III and the constraints on the leptoquark parameter space has been obtained by using the measured branching ratios of the rare decays $B_s \to l^+ l^-$. In section IV, we present the numerical analysis for the branching ratios and other physical observables such as the forward-backward asymmetry, lepton polarization asymmetry and the lepton non-universality by using the constrained leptoquark couplings. We compute the branching ratios of the lepton flavour violating $\Lambda_b \to \Lambda l_i^- l_j^+$ decays in section V and section VI contains the summary and conclusion.

II. THEORETICAL FRAMEWORK FOR THE ANALYSIS OF $\Lambda_b \to \Lambda l^+ l^-$ DECAY PROCESS

In this section, we will discuss the SM contributions to the branching ratios and other physical observables of the $\Lambda_b \to \Lambda l^+ l^-$, $l = e, \mu, \tau$ processes. The effective Hamiltonian describing the decay process $\Lambda_b \to \Lambda l^+ l^-$ involves the quark level transition $b \to s l^+ l^-$ and is given by [38]

$$\begin{aligned} \mathcal{H}_{eff} \;=\; & -\frac{4G_F}{\sqrt{2}} V_{tb} V_{ts}^* \Bigg[\sum_{i=1}^{6} C_i(\mu) O_i + C_7 \frac{e}{16\pi^2} \Big(\bar{s} \sigma_{\mu\nu} (m_s P_L + m_b P_R) b \Big) F^{\mu\nu} \\ & + C_9^{eff} \frac{\alpha}{4\pi} (\bar{s} \gamma^\mu P_L b) \bar{l} \gamma_\mu l + C_{10} \frac{\alpha}{4\pi} (\bar{s} \gamma^\mu P_L b) \bar{l} \gamma_\mu \gamma_5 l \Bigg] \,, \end{aligned} \tag{1}$$

where $V_{qq'}$ are the CKM matrix elements, G_F denotes the Fermi constant, α is the fine-structure constant, C_i's are the Wilson coefficients evaluated at the renormalized scale $\mu = m_b$ [39] and $P_L, P_R = (1 \mp \gamma_5)/2$ are the chiral operators. The sum over i includes the current-current operators $i = 1, 2$ and the QCD-penguin operators $i = 3, 4, 5, 6$.

In addition to the short distance contributions these processes also receive additional contributions arising from the long distance effects due to the real $c\bar{c}$ resonant states of $J/\psi, \psi'$, i.e., $\Lambda_b \to \Lambda J/\psi(\psi') \to \Lambda l^+ l^-$. These resonance contributions can be included by modifying the Wilson coefficient C_9. Thus, the modified coefficient (C_9^{eff}) contains a perturbative part and a resonance part which can be written as

$$C_9^{eff} = C_9^{SM} + Y(s) + C_9^{res} \,, \tag{2}$$

where C_9^{SM} is the SM Wilson coefficient evaluated at the b quark mass scale [39], the perturbative part $Y(s)$ receives contributions coming from one-loop matrix elements of the four quark operators [40] and the long distance resonance effect is given by [41]

$$C_9^{res} = \frac{3\pi}{\alpha^2}(3C_1 + C_2 + 3C_3 + C_4 + 3C_5 + C_6) \sum_{V_i=\psi(1S),\cdots,\psi(6S)} \kappa_{V_i} \frac{m_{V_i}\Gamma(V_i \to l^+l^-)}{m_{V_i}^2 - s - i m_{V_i}\Gamma_{V_i}} \ . \quad (3)$$

Here the phenomenological parameter κ is taken to be 1.65 and 2.36 [42] for the lowest resonances J/ψ and ψ' respectively in order to reproduce the correct branching ratio of $\mathcal{B}(B \to J/\psi K^* \to K^* l^+ l^-) = \mathcal{B}(B \to J/\psi K^*)\mathcal{B}(J/\psi \to l^+ l^-)$.

The matrix elements of the hadronic currents in (1) between initial Λ_b and the final Λ baryon can be parameterized in terms of various form factors which are presented in Appendix A. Thus, using these matrix elements, the transition amplitude for the $\Lambda_b \to \Lambda l^+ l^-$ processes can be written as [16, 18]

$$\begin{aligned}
\mathcal{M}(\Lambda_b \to \Lambda l^+ l^-) \ = \ & \frac{G_F\ \alpha}{\sqrt{2}\pi} V_{tb}V_{ts}^* \Bigg[\bar{l}\gamma_\mu l \Big\{ \bar{u}_\Lambda \Big(\gamma^\mu (A_1 P_R + B_1 P_L) + i\sigma^{\mu\nu} q_\nu (A_2 P_R + B_2 P_L) \Big) u_{\Lambda_b} \Big\} \\
& + \ \bar{l}\gamma_\mu\gamma_5 l \Big\{ \bar{u}_\Lambda \Big(\gamma^\mu (D_1 P_R + E_1 P_L) + i\sigma^{\mu\nu} q_\nu (D_2 P_R + E_2 P_L) \\
& + \ q^\mu (D_3 P_R + E_3 P_L) \Big) u_{\Lambda_b} \Big\} \Bigg] \ , \qquad (4)
\end{aligned}$$

where the parameters A_i, B_i, D_j and E_j with $i = 1, 2$, $j = 1, 2, 3$ are defined as

$$\begin{aligned}
A_i \ &= \ C_9^{eff} \frac{f_i - g_i}{2} - \frac{2m_b}{q^2} C_7 \frac{f_i^T + g_i^T}{2}, \\
B_i \ &= \ C_9^{eff} \frac{f_i + g_i}{2} - \frac{2m_b}{q^2} C_7 \frac{f_i^T - g_i^T}{2}, \\
D_j \ &= \ C_{10} \frac{f_j - g_j}{2}, \\
E_j \ &= \ C_{10} \frac{f_j + g_j}{2}. \qquad (5)
\end{aligned}$$

Using the transition amplitude (4), the double differential decay rate is given by

$$\frac{d^2\Gamma}{d\hat{s}\ dz} = \frac{G_F^2\ \alpha^2}{2^{12}\pi^5} \ |V_{tb}V_{ts}^*|^2 \ m_{\Lambda_b}\ v_l\ \lambda^{1/2}(1, r, \hat{s})\ \mathcal{K}(\hat{s}, z) \ , \qquad (6)$$

where

$$\mathcal{K}(\hat{s}, z) = \mathcal{K}_0(\hat{s}) + z\ \mathcal{K}_1(\hat{s}) + z^2\ \mathcal{K}_2(\hat{s}) \ , \qquad (7)$$

$\hat{s} = s/m_{\Lambda_b}^2$ and $z = \hat{p}_B \cdot \hat{p}_l^+$ is the angle between the momenta of Λ_b and l^+ in the dilepton invariant mass frame. The complete expressions for $\mathcal{K}_0(\hat{s})$, $\mathcal{K}_1(\hat{s})$ and $\mathcal{K}_2(\hat{s})$ are given in

Appendix B. Here $v_l = \sqrt{1-(4m_l^2/q^2)}$ and $\lambda(1,r,\hat{s}) = (1-r)^2 - 2\hat{s}(1+r) + \hat{s}^2$ is the triangle function with $r = m_\Lambda/m_{\Lambda_b}$. The physical allowed range for $s \equiv q^2$ is

$$4m_l^2 \leq s \leq (m_{\Lambda_b} - m_\Lambda)^2 \,. \tag{8}$$

Another interesting observable is the zero-crossing of the forward-backward asymmetry, wherein the position of the zero value of the forward-backward asymmetry parameter (A_{FB}) is very useful to look for the new physics signal. The normalized forward-backward asymmetry is defined as

$$A_{FB}(\hat{s}) = \frac{\displaystyle\int_0^1 \frac{d^2\Gamma}{d\hat{s}dz}dz - \int_{-1}^0 \frac{d^2\Gamma}{d\hat{s}dz}dz}{\displaystyle\int_0^1 \frac{d^2\Gamma}{d\hat{s}dz}dz + \int_{-1}^0 \frac{d^2\Gamma}{d\hat{s}dz}dz}, \tag{9}$$

which can be simplified to

$$A_{FB}(\hat{s}) = \frac{\mathcal{K}_1(\hat{s})}{\mathcal{K}_0(\hat{s}) + \mathcal{K}_2(\hat{s})/3} \,. \tag{10}$$

The polarization asymmetries P_i $(i = L, N, T)$ are defined as

$$P_i(\hat{s}) = \frac{\dfrac{d\Gamma}{d\hat{s}}(\hat{\eta} = \hat{e}_i) - \dfrac{d\Gamma}{d\hat{s}}(\hat{\eta} = -\hat{e}_i)}{\dfrac{d\Gamma}{d\hat{s}}(\hat{\eta} = \hat{e}_i) + \dfrac{d\Gamma}{d\hat{s}}(\hat{\eta} = -\hat{e}_i)} \,, \tag{11}$$

where $\hat{e}_i$'s are the unit vectors along the longitudinal, normal and transverse components of the l^+ polarization and $\hat{\eta}$ is a unit vector, used to write the l^+ four-spin vector (s_+), along the l^+ spin in its rest frame as

$$s_+^0 = \frac{\vec{p}_+ \cdot \hat{\eta}}{m_l} \,, \quad \vec{s}_+ = \hat{\eta} + \frac{s_+^0}{E_{l^+} + m_l}\vec{p}_+ \,. \tag{12}$$

Thus, the observables P_L, P_T and P_N correspond to longitudinal, transverse and normal polarization asymmetries respectively. The observables P_L and P_T are P-odd, T-even, while P_N is P-even, T-odd and CP-odd. The explicit expressions for forward-backward asymmetry and all the polarization parameters are taken from [16, 18, 19].

Another interesting observable is the lepton universality violation (LUV) parameter, which has been recently observed by the LHCb collaboration in $B^+ \to K^+ l^+ l^-$ process and has 2.6σ deviation from its SM predicted value [6]. Analogously, we define the parameter (R_Λ) as the ratio of branching fractions of $\Lambda_b \to \Lambda l^+ l^-$ into dimuon over dielectron as

$$R_\Lambda = \frac{\mathrm{Br}(\Lambda_b \to \Lambda \mu^+ \mu^-)}{\mathrm{Br}(\Lambda_b \to \Lambda e^+ e^-)}. \tag{13}$$

III. NEW PHYSICS CONTRIBUTION DUE TO SCALAR LEPTOQUARK EXCHANGE

In this section we will consider the effect of scalar leptoquarks to the $\Lambda_b \to \Lambda l^+ l^-$ decay processes. The exchange of leptoquarks will contribute additional operators to the SM effective Hamiltonian and thus, the various observables may deviate significantly from their corresponding SM values. The scalar leptoquark multiplets with representations $X(3,2,7/6)$ and $X(3,2,1/6)$ under the SM gauge group $SU(3)_C \times SU(2)_L \times U(1)_Y$ conserve baryon and lepton numbers and don't allow proton decay. These baryon and lepton number conserving scalar leptoquarks can have sizable Yukawa couplings and could be light enough to be accessible in accelerator searches. Thus, they could potentially contribute to the $b \to s l^+ l^-$ transitions and one can constrain the underlying couplings from experimental data on $B_s \to l^+ l^-$ processes as well as from $B_s - \bar{B}_s$ mixing.

The interaction Lagrangian of the scalar leptoquarks $X = (3,2,7/6)$ with the SM bilinear fermions is given as [33, 34]

$$\mathcal{L} = -\lambda_u^{ij}\ \bar{u}_R^i X^T \epsilon L_L^j - \lambda_e^{ij}\ \bar{e}_R^i X^\dagger Q_L^j + h.c., \tag{14}$$

where i, j are the generation indices, X is the leptoquark doublet, Q_L (L_L) denotes the left handed quark (lepton) doublet, the right handed up-type quark (charged lepton) singlet is represented by u_R (e_R) and $\epsilon = i\sigma_2$ is a 2×2 matrix. The multiplets defined above are represented as

$$X = \begin{pmatrix} V_\alpha \\ Y_\alpha \end{pmatrix}, \qquad Q_L = \begin{pmatrix} u_L \\ d_L \end{pmatrix}, \qquad \text{and} \qquad L_L = \begin{pmatrix} \nu_L \\ e_L \end{pmatrix}. \tag{15}$$

Now expanding the $SU(2)$ indices, the interaction Lagrangian (14) takes the form

$$\mathcal{L} = -\lambda_u^{ij}\ \bar{u}_{\alpha R}^i (V_\alpha e_L^j - Y_\alpha \nu_L^j) - \lambda_e^{ij}\ \bar{e}_R^i \left(V_\alpha^\dagger u_{\alpha L}^j + Y_\alpha^\dagger d_{\alpha L}^j\right) + h.c.\ . \tag{16}$$

Thus, from Eq. (16) one can obtain the interaction Hamiltonian for $b \to s l_i^+ l_i^-$ processes after performing the Fierz transformation as

$$\mathcal{H}_{LQ} = \frac{\lambda_e^{i3}\lambda_e^{i2*}}{8M_Y^2}[\bar{s}\gamma^\mu(1-\gamma_5)b][\bar{l}_i\gamma_\mu(1+\gamma_5)l_i] = \frac{\lambda_e^{i3}\lambda_e^{i2*}}{4M_Y^2}(O_9 + O_{10})\ . \tag{17}$$

Comparing (17) with the corresponding SM effective Hamiltonian (1), one can obtain the new Wilson coefficients as

$$C_9^{NP} = C_{10}^{NP} = -\frac{\pi}{2\sqrt{2}G_F\alpha V_{tb}V_{ts}^*}\frac{\lambda_e^{i3}\lambda_e^{i2*}}{M_Y^2}\ . \tag{18}$$

Similarly, the interaction Lagrangian due to the exchange of the scalar leptoquark $X = (3, 2, 1/6)$ is

$$\mathcal{L} = -\lambda_d^{ij}\ \bar{d}^i_{\alpha R}(V_\alpha e^j_L - Y_\alpha \nu^j_L) + h.c.\ , \tag{19}$$

which contributes to the primed Wilson coefficients ($C'_{9,10}$) corresponding to the semileptonic electroweak penguin operators $\mathcal{O}'_{9,10}$ (i.e., the right-handed counter parts of the SM operators $\mathcal{O}_{9,10}$) and are given as

$$C_9^{\prime NP} = -C_{10}^{\prime NP} = \frac{\pi}{2\sqrt{2}\ G_F \alpha V_{tb} V_{ts}^*} \frac{\lambda_s^{2i} \lambda_b^{3i*}}{M_V^2}\ . \tag{20}$$

Thus, from the above Eqs. (18) and (20), one can find that there are four additional Wilson coefficients $C_{9,10}^{(\prime)NP}$, which will contribute to the $b \to s l^+ l^-$ processes due to the scalar leptoquark exchange. Thus, the modified parameters (5) in the amplitude (4), become

$$\begin{aligned}
A_i &= C_9^{\prime NP} \frac{f_i + g_i}{2} + (C_9^{eff} + C_9^{NP}) \frac{f_i - g_i}{2} - \frac{2m_b}{q^2} C_7^{SM} \frac{f_i^T + g_i^T}{2}, \\
B_i &= (C_9^{eff} + C_9^{NP}) \frac{f_i + g_i}{2} - \frac{2m_b}{q^2} C_7^{SM} \frac{f_i^T - g_i^T}{2} + C_9^{\prime NP} \frac{f_i - g_i}{2}, \\
D_j &= C_{10}^{\prime NP} \frac{f_j + g_j}{2} + (C_{10}^{SM} + C_{10}^{NP}) \frac{f_j - g_j}{2}, \\
E_j &= (C_{10}^{SM} + C_{10}^{NP}) \frac{f_j + g_j}{2} + C_{10}^{\prime NP} \frac{f_j - g_j}{2}.
\end{aligned} \tag{21}$$

Next, we have to find out the constraints on the leptoquark couplings to see how various observables behave in the LQ model. The detailed calculation of the constraint on the new leptoquark parameter space has been presented in [29–31], therefore here we will simply quote the main results. We constrain the leptoquark coupling by comparing the theoretical [44] and experimental [45–47] branching ratios of $B_s \to l^+ l^-$ processes and the $B_s - \bar{B}_s$ mixing data [8]. For completeness, here we briefly outline the procedure for obtaining the constraints from $B_s \to \mu^+ \mu^-$ process and $B_s - \bar{B}_s$ mixing, however, the technical details can be found in [29–31].

A. Constraint from $B_s \to \mu^+\mu^-$ process

In the leptoquark model the branching ratio for the $B_s \to \mu^+\mu^-$ mode can be given as

$$\begin{aligned}\mathrm{Br}(B_s \to \mu^+\mu^-) &= \frac{G_F^2}{16\pi^3}\tau_{B_s}\alpha^2 f_{B_s}^2 M_{B_s} m_\mu^2 |V_{tb}V_{ts}^*|^2 \left|C_{10}^{SM} + C_{10}^{NP} - C_{10}^{\prime NP}\right|^2 \sqrt{1-\frac{4m_\mu^2}{M_{B_s}^2}} \\ &= \mathrm{Br}^{SM}\left|1 + \frac{C_{10}^{NP} - C_{10}^{\prime NP}}{C_{10}^{SM}}\right|^2 \equiv \mathrm{Br}^{SM}\left|1 + re^{i\phi^{NP}}\right|^2 , \end{aligned} \tag{22}$$

where Br^{SM} is the SM branching ratio and the parameters r and ϕ^{NP} are defined as

$$re^{i\phi^{NP}} = \frac{C_{10}^{NP} - C_{10}^{\prime NP}}{C_{10}^{SM}} . \tag{23}$$

Now comparing the SM theoretical prediction of $\mathrm{Br}(B_s \to \mu^+\mu^-)$ [44]

$$\mathrm{Br}(B_s \to \mu^+\mu^-)|_{\mathrm{SM}} = (3.65 \pm 0.23) \times 10^{-9}, \tag{24}$$

with the corresponding experimental value [45–47]

$$\mathrm{Br}(B_s \to \mu^+\mu^-) = (2.9 \pm 0.7) \times 10^{-9}, \tag{25}$$

and assuming that each individual leptoquark contribution to the branching ratio does not exceed the experimental result, one can obtain the bound on the new physics parameters r and ϕ^{NP}. The allowed parameter space in $r - \phi^{NP}$ plane which is compatible with the 1σ range of the experimental data is

$$0 \le r \le 0.35 , \quad \text{with} \quad \pi/2 \le \phi^{NP} \le 3\pi/2 . \tag{26}$$

These bounds can be translated to obtain the bounds for the leptoquark couplings as

$$0 \le \frac{|\lambda_\mu^{23}\lambda_\mu^{22*}|}{M_Y^2} = \frac{|\lambda_s^{22}\lambda_b^{32*}|}{M_V^2} \le 5 \times 10^{-9}\ \mathrm{GeV}^{-2} \quad \text{for} \quad \pi/2 \le \phi^{NP} \le 3\pi/2 . \tag{27}$$

Similarly, one can obtain the upper bound on the product of various combination of leptoquark couplings from $B_s \to l^+l^-$ processes which are presented in Table I. Using the bounds on leptoquark couplings one can obtain the constraints on new Wilson coefficients using the eqns. (18) and (20).

TABLE I: Constraints on the leptoquark couplings obtained from various leptonic $B_s \to l^+ l^-$ decays [29], where M_S denotes the mass of the scalar LQ.

Decay Process	Couplings involved	Bound on the LQ couplings (GeV^{-2})
$B_s \to \mu^\pm \mu^\mp$	$\frac{\lvert\lambda^{32}\lambda^{22*}\rvert}{M_S^2}$	$< 5.0 \times 10^{-9}$
$B_s \to e^\pm e^\mp$	$\frac{\lvert\lambda^{31}\lambda^{21*}\rvert}{M_S^2}$	$< 2.54 \times 10^{-5}$
$B_s \to \tau^\pm \tau^\mp$	$\frac{\lvert\lambda^{33}\lambda^{23*}\rvert}{M_S^2}$	$< 1.2 \times 10^{-8}$

B. Constraint from $B_s - \bar{B}_s$ mixing

In this subsection, we will discuss the constraint on leptoquark couplings from the $B_s - \bar{B}_s$ mixing, which in the SM, proceeds through the box diagram with internal top quark and W boson exchange. The effective Hamiltonian describing the $\Delta B = 2$ transition is given as [48]

$$\mathcal{H}_{eff} = \frac{G_F^2}{16\pi^2} \ |V_{tb}V_{ts}^*|^2 \ M_W^2 S_0(x_t) \eta_B (\bar{s}b)_{V-A} (\bar{s}b)_{V-A} \ , \tag{28}$$

where η_B is the QCD correction factor and $S_0(x_t)$ is the loop function given in Ref. [48]. Thus, the $B_s - \bar{B}_s$ mixing amplitude in the SM, can be written as

$$M_{12}^{SM} = \frac{1}{2M_{B_s}} \langle \bar{B}_s | \mathcal{H}_{eff} | B_s \rangle = \frac{G_F^2}{12\pi^2} M_W^2 \ |V_{tb}V_{ts}^*|^2 \ \eta_B \ \hat{B}_s f_{B_s}^2 M_{B_s} S_0(x_t) \ . \tag{29}$$

The corresponding mass difference can be computed from the mixing amplitude through $\Delta M_s = 2|M_{12}|$. Now using the particle masses from [8], $\eta_B = 0.551$, the Bag parameter $\hat{B}_{B_s} = 1.320 \pm 0.017 \pm 0.030$ and the decay constant $f_{B_s} = 225.6 \pm 1.1 \pm 5.4$ from [49], the value of ΔM_s in the SM, is found as

$$\Delta M_s^{SM} = (17.426 \pm 1.057) \ \text{ps}^{-1}, \tag{30}$$

which is in good agreement with the experimental result [8]

$$\Delta M_s = 17.761 \pm 0.022 \ \text{ps}^{-1}. \tag{31}$$

For $X(3, 2, 7/6)$ LQ, the mixing amplitude receives additional contribution from leptoquark and charged lepton in the box diagram whereas for $X(3, 2, 1/6)$ both charged lepton and

neutrino will contribute to the mixing amplitude. The effective Hamiltonian due to the leptoquark $X(3,2,7/6)$ is given by

$$\mathcal{H}_{eff} = \sum_{i=e,\mu,\tau} \frac{(\lambda^{bi}\lambda^{si*})^2}{128\pi^2} \frac{1}{M_S^2}\, I\left(\frac{m_i^2}{M_S^2}\right) (\bar{b}\gamma^\mu P_L s)(\bar{b}\gamma_\mu P_L s)\ , \tag{32}$$

and for $X(3,2,1/6)$ leptoquark the corresponding effective Hamiltonian becomes

$$\mathcal{H}_{eff} = \sum_{i=e,\mu,\tau} \frac{(\lambda^{bi*}\lambda^{si})^2}{128\pi^2} \left[\frac{1}{M_S^2}\, I\left(\frac{m_i^2}{M_S^2}\right) + \frac{1}{M_S^2}\right] (\bar{b}\gamma^\mu P_R s)(\bar{b}\gamma_\mu P_R s)\ . \tag{33}$$

where the loop function $I(x)$ is given as

$$I(x) = \frac{1 - x^2 + 2x\log x}{(1-x)^2}. \tag{34}$$

Thus, the contribution to the mixing amplitude due to the exchange of scalar leptoquark is given by

$$\begin{aligned} M_{12}^{LQ} &= \frac{(\lambda^{32*}\lambda^{22})^2}{192\pi^2 M_S^2}\eta_B \hat{B}_{B_s} f_{B_s}^2 M_{B_s}\ , \qquad \text{for } X(3,2,1/6) \\ M_{12}^{LQ} &= \frac{(\lambda^{32}\lambda^{22*})^2}{384\pi^2 M_S^2}\eta_B \hat{B}_{B_s} f_{B_s}^2 M_{B_s}\ , \qquad \text{for } X(3,2,7/6). \end{aligned} \tag{35}$$

Including both the SM and leptoquark contributions the total mass difference is given as

$$\Delta M_s = \Delta M_s^{SM} \left|\left[1 + \frac{c}{16 G_F^2 |V_{tb}V_{ts}^*|^2 m_W^2 S_0(x_t)} \left(\frac{(\lambda^{32}\lambda^{22*})^2}{M_S^2}\right)\right]\right|\ , \tag{36}$$

where the constant $c = 1$ for $X(3,2,1/6)$ and $1/2$ for $X(3,2,7/6)$. Now varying the mass difference $(\Delta M_s/\Delta M_s^{SM})$ within its 1σ allowed range [8], the constraint on $|\lambda^{32}\lambda^{22}/M_S|$ is found to be [31]

$$\begin{aligned} 0 \le \left|\frac{\lambda^{32}\lambda^{22}}{M_S}\right| &\le 7.5\times 10^{-5}\ \text{GeV}^{-1}\ , \qquad \text{for } X(3,2,7/6), \\ 0 \le \left|\frac{\lambda^{32}\lambda^{22}}{M_S}\right| &\le 5.0\times 10^{-5}\ \text{GeV}^{-1}\ , \qquad \text{for } X(3,2,1/6). \end{aligned} \tag{37}$$

In order to relate this results with the bounds obtained $B_s \to \mu\mu$ process, we scale the couplings obtained from $B_s - \bar{B}_s$ mass difference for a benchmark leptoquark mass of 1 TeV and the bounds in Eq. (37) is translated as

$$\begin{aligned} 0 \le \left|\frac{\lambda^{32}\lambda^{22}}{M_S^2}\right| &\le 7.5\times 10^{-8}\ \text{GeV}^{-2}, \qquad \text{for } X(3,2,7/6) \\ 0 \le \left|\frac{\lambda^{32}\lambda^{22}}{M_S^2}\right| &\le 5.0\times 10^{-8}\ \text{GeV}^{-2}, \qquad \text{for } X(3,2,1/6), \end{aligned} \tag{38}$$

which are reasonably higher than those of obtained from $B_s \to \mu\mu$ process. Hence in our analysis, we will use the bounds (26) as discussed in the previous subsection.

IV. NUMERICAL ANALYSIS

After having the detailed knowledge about the SM observables and the bound on the new leptoquark couplings, we now proceed for numerical analysis. We have taken the particle masses and the life time of Λ_b baryon from [8]. The q^2 dependence of form factors derived

TABLE II: Numerical values of the form factor $f_1(0)$, $f_2(0)$ and the parameters involved in the double fit for $\Lambda_b \to \Lambda$ transition.

Parameter	LCSR (twist-3) [21]
$f_1(0)$	$0.14^{+0.02}_{-0.01}$
a	$2.91^{+0.1}_{-0.07}$
b	$2.26^{+0.13}_{-0.08}$
$f_2(0)$ $(10^{-2}$ GeV$^{-1})$	$-0.47^{+0.06}_{-0.06}$
a	$3.4^{+0.06}_{-0.05}$
b	$2.98^{+0.09}_{-0.08}$

in the light cone sum rule (LCSR) approach can be parameterized as

$$f_i(q^2) = \frac{f_i(0)}{1 - a(q^2/m^2_{\Lambda_b}) + b(q^2/m^2_{\Lambda_b})^2}, \tag{39}$$

where the values of the parameters $f_i(0)$, a and b and are listed in Table II [21]. The other form factors are related to these two and the HQET form factors ($F_{1,2}$) through [21]

$$\begin{aligned} f_2^T &= g_2^T = f_1 = g_1 = F_1 + \frac{m_\Lambda}{m_{\Lambda_b}} F_2, \\ f_2 &= g_2 = f_3 = g_3 = \frac{F_2}{m_{\Lambda_b}}, \\ f_1^T &= g_1^T = \frac{F_2}{m_{\Lambda_b}} q^2. \end{aligned} \tag{40}$$

In the lattice QCD formalism, the $\Lambda_b \to \Lambda$ helicity form factors, i.e., $f_{+,\perp,0}$, $g_{+,\perp,0}$, $h_{+,\perp}$ and $\tilde{h}_{+,\perp}$ in the physical limit can have the simple form [23]

$$f(q^2) = \frac{1}{1 - q^2/(m^f_{pole})^2} \Big[a_0^f + a_1^f z(q^2) + a_2^f [z(q^2)]^2 \Big], \tag{41}$$

where the values and uncertainties of the parameters a_0^f, a_1^f and a_2^f from the higher-order fit are given in Table V of [23]. These helicity form factors are related to the form factors $f_i^{(T)}$ and $g_i^{(T)}$ used in this work as follows:

$$\begin{aligned}
f_+ &= f_1 - \frac{q^2}{m_{\Lambda_b}+m_\Lambda} f_2, \qquad f_\perp = f_1 - (m_{\Lambda_b}+m_\Lambda) f_2, \qquad f_0 = f_1 + \frac{q^2}{m_{\Lambda_b}-m_\Lambda} f_3, \\
g_+ &= g_1 + \frac{q^2}{m_{\Lambda_b}-m_\Lambda} g_2, \qquad g_\perp = g_1 + (m_{\Lambda_b}-m_\Lambda) g_2, \qquad g_0 = g_1 - \frac{q^2}{m_{\Lambda_b}+m_\Lambda} g_3, \\
h_+ &= f_2^T - \frac{m_{\Lambda_b}+m_\Lambda}{q^2} f_1^T, \qquad h_\perp = f_2^T - \frac{f_1^T}{m_{\Lambda_b}+m_\Lambda}, \\
\tilde{h}_+ &= g_2^T + \frac{m_{\Lambda_b}-m_\Lambda}{q^2} g_1^T, \qquad \tilde{h}_\perp = g_2^T + \frac{g_1^T}{m_{\Lambda_b}-m_\Lambda}.
\end{aligned} \tag{42}$$

In our analysis, we have taken the form factors computed in the light cone sum rule approach for low q^2 region (as these are not so well-behaved in the high q^2 regime), and for high q^2 theory we have used the lattice QCD calculations of $\Lambda_b \to \Lambda$ form factors [23]. The values of the Wilson coefficients used in our analysis are evaluated at the renormalization scale $\mu \approx m_b = 4.8$ GeV. In the LQ model, the new physics contributions to the branching ratios and forward-backward asymmetry parameters are encoded in the new Wilson coefficients. By using the above input parameters and the values of the new Wilson coefficients, we show in Fig. 1, the q^2 variation of branching ratio of $\Lambda_b \to \Lambda e^+ e^-$ (top left panel), $\Lambda_b \to \Lambda \mu^+ \mu^-$ (top right panel) and $\Lambda_b \to \Lambda \tau^+ \tau^-$ (bottom panel) processes for the full kinematically accessible physical region. In these plots, we have shown the contributions arising from the exchange of $X = (3, 2, 7/6)$ leptoquark. The SM contributions are represented by blue lines and the grey bands denote the theoretical uncertainties arising due to the uncertainties associated with the CKM matrix elements and the hadronic form factors. The green bands represent the leptoquark contributions to the branching ratios. The bin-wise experimental results for $\Lambda_b \to \Lambda \mu^+ \mu^-$ process [15] are shown by black data points. There is slight deviation in the decay distribution between the predicted and observed data. The corresponding results coming from the exchange of the $X = (3, 2, 1/6)$ LQ are shown in Fig. 2. From these figures, one can see that the branching ratios of $\Lambda_b \to \Lambda e^+ e^-$ and $\Lambda_b \to \Lambda \tau^+ \tau^-$ decay processes deviate significantly from their SM predictions, whereas the new physics effects on $\Lambda_b \to \Lambda \mu^+ \mu^-$ branching ratio is not so prominent. In Table III, we present the integrated values of branching ratio for all the above processes, where we have used the veto windows as ($8\ \text{GeV}^2 < m^2_{l^+l^-} < 11\ \text{GeV}^2$) and ($12.5\ \text{GeV}^2 < m^2_{l^+l^-} < 15\ \text{GeV}^2$) [15],

to eliminate the backgrounds coming from the dominant resonances $\Lambda_b \to \Lambda J/\psi(\psi')$ with $J/\psi(\psi') \to l^+l^-$. The predicted branching ratio for $\Lambda_b \to \Lambda\mu^+\mu^-$ is almost consistent with the observed data $\mathrm{Br}(\Lambda_b \to \Lambda\mu^+\mu^-) = (1.08 \pm 0.28) \times 10^{-6}$ [8]. Also, as seen from Table III, the experimental result can be accommodated in the leptoquark model. Within the SM, the forward backward asymmetry parameters in the $B \to Kl^+l^-$ decay processes are identically zero since they only involve scalar and tensor types of currents, whereas $B \to Kl^+l^-$ processes are described by only vector-type interactions. However, for semileptonic $\Lambda_b \to \Lambda l^+l^-$ decay processes, the forward backward asymmetry depends on two combinations of the Wilson coefficients $\mathrm{Re}(C_7^{eff}C_{10}^*)$ and $\mathrm{Re}(C_9^{eff}C_{10}^*)$ [16] and thus, can have negative values in the SM. The contribution due to the new Wilson coefficients ($C_{9,10}^{NP(\prime)}$) may enhance the rate of asymmetries and can shift the zero position of these asymmetries. In Fig. 3, the variation of forward-backward asymmetry for $\Lambda_b \to \Lambda\mu^+\mu^-$ (left panel), $\Lambda_b \to \Lambda\tau^+\tau^-$ (right panel) modes are depicted with respect to q^2 both in the SM and in the $X = (3, 2, 7/6)$ LQ model including the LD contributions and the corresponding integrated values are presented in Table III. Similarly the variation of forward-backward asymmetries for $X = (3, 2, 1/6)$ LQ exchange are shown in Fig. 4. We found no significant deviation of the zero position of A_{FB} from its SM value due to the leptoquark contributions in $\Lambda_b \to \Lambda\mu^+\mu^-$ process. However, there is certain discrepancy between the observed and predicted results in the high q^2 regime. The forward-backward asymmetry for $\Lambda_b \to \Lambda\tau^+\tau^-$ process however, has significant deviation from the SM in both the $X = (3, 2, 7/6)$ and $X = (3, 2, 1/6)$ leptoquark model. Besides the branching ratios and forward-backward asymmetry parameters of $\Lambda_b \to \Lambda l^+l^-$ processes, the new physics effects can also be observed in the lepton polarization asymmetries. In the left panel of Fig. 5, the distribution of the longitudinal (top), transverse (middle) and normal (bottom) polarization components for $\Lambda_b \to \Lambda\mu^+\mu^-$ process are shown both in the SM and in the $X = (3, 2, 7/6)$ LQ model, and the corresponding plots for $\Lambda_b \to \Lambda\tau^+\tau^-$ process are presented in the right panel. The integrated values of all the three polarizations in the full physical phase space have been presented in Table III. In Fig. 6, we have shown the variation of the different polarization parameters for $\Lambda_b \to \Lambda\mu^+\mu^-$ process in the $X = (3, 2, 1/6)$ leptoquark model. It is found from Table III, that the transverse and normal polarization values are very small in the SM and even the leptoquark model does not give any significant deviation.

Analogous to the lepton flavour non-universality parameter R_K, i.e., the ratio of branching

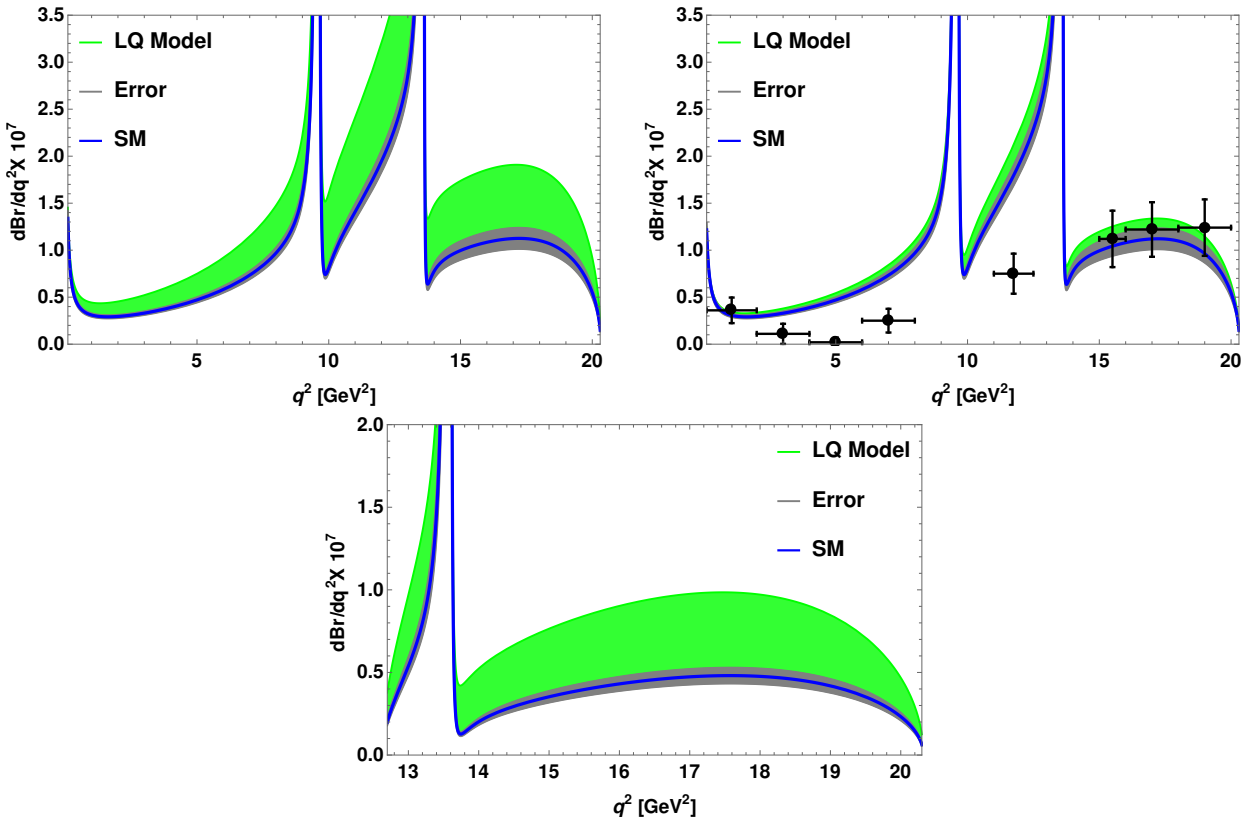

FIG. 1: The variation of branching ratio of $\Lambda_b \to \Lambda e^+ e^-$ (left panel), $\Lambda_b \to \Lambda \mu^+ \mu^-$ (right panel) and $\Lambda_b \to \Lambda \tau^+ \tau^-$ (bottom panel) with respect to low and high q^2 including the LD contributions, both in the SM and in the $X = (3, 2, 7/6)$ leptoquark model. In each plot, the green band represents the leptoquark contribution and the blue solid line is for the SM. The grey band represents the theoretical uncertainty arises due to the input parameters in the SM. The black data points in $\Lambda_b \to \Lambda \mu^+ \mu^-$ process represent the bin-wise experimental data.

fractions of $B \to K \mu^+ \mu^-$ over $B \to K e^+ e^-$, we would like to see whether it is possible to observe lepton non-universality in the Λ_b decays. We have define these parameters as e.g., $R_\Lambda^{\mu e} = \text{Br}(\Lambda_b \to \Lambda \mu^+ \mu^-)/\text{Br}(\Lambda_b \to \Lambda e^+ e^-)$. In Fig. 7, we show the variation of lepton nonuniversality parameter $R_\Lambda^{\mu e}$ (top-right panel), $R_\Lambda^{\tau e}$ (bottom-left panel) and $R_\Lambda^{\tau \mu}$ (bottom-right panel) in their respective q^2 region. Also, we show the low-q^2 behavior of $R_\Lambda^{\mu e}$ (top-left panel), in the range $1 \leq q^2 \leq 6$ GeV^2. These results are for $X = (3, 2, 7/6)$ leptoquark. Similarly the lepton nonuniversality plot for $X = (3, 2, 1/6)$ leptoquark exchange is shown in Fig. 8. The integrated values of the lepton non-universality parameter in both SM and LQ model are presented in Table III. We found that there is significant violation of

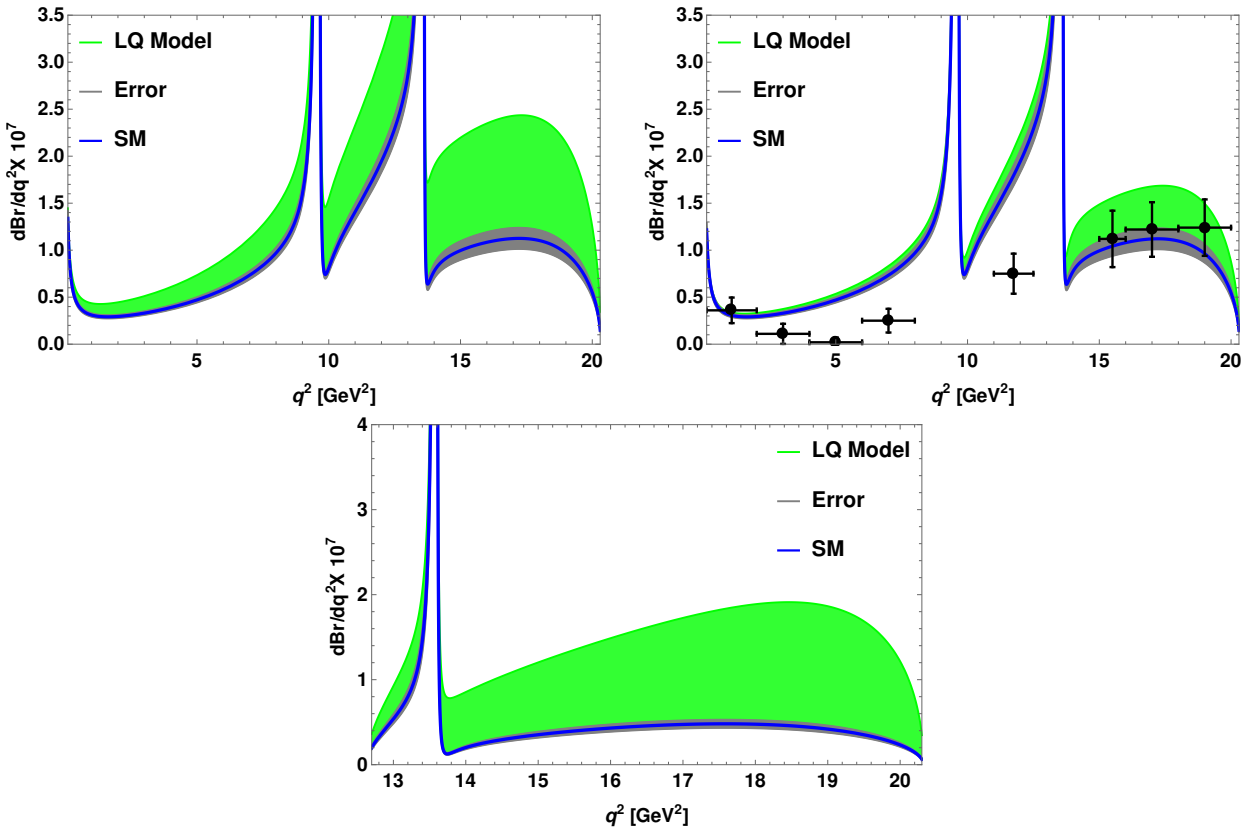

FIG. 2: Same as Fig.1 for $X = (3, 2, 1/6)$ LQ exchange.

lepton universality in Λ_b decays, though there is no experimental evidence so far. The violation of lepton universality is more pronounced for the processes having τ as final particle. However, as the reconstruction of tau events are extremely difficult, this observable may not be sensitive enough to be observed in near future. As seen from the top-left panel of Figs. 7 and 8, the parameter $R_\Lambda^{\mu e}$ is very promising for the Belle II experiment, as the LHCb, being a hadronic machine works better in muon mode than electron.

V. LEPTON FLAVOUR VIOLATING $\Lambda_b \to \Lambda l_i^- l_j^+$ DECAYS

In this section, we will compute the branching ratios of lepton flavour violating (LFV) Λ_b decays mediating through the exchange of scalar leptoquarks. The LFV decay processes are extremely rare in the SM as they are either two-loop suppressed with tiny neutrino masses in one of the loop or proceed through box diagram (which is also highly suppressed due to tiny neutrino mass). However, they can occur at tree level in the LQ model and

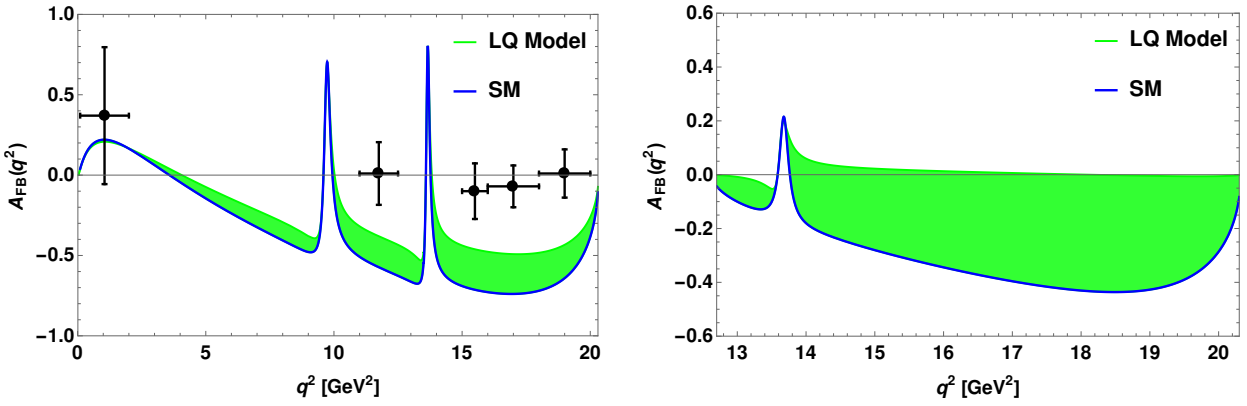

FIG. 3: The forward-backward asymmetry variation of $\Lambda_b \to \Lambda\mu^+\mu^-$ (left panel) and $\Lambda_b \to \Lambda\tau^+\tau^-$ (right panel) with respect to q^2 for $X = (3, 2, 7/6)$ LQ exchange. The black data points in $\Lambda_b \to \Lambda\mu^+\mu^-$ process represent the bin-wise experimental data.

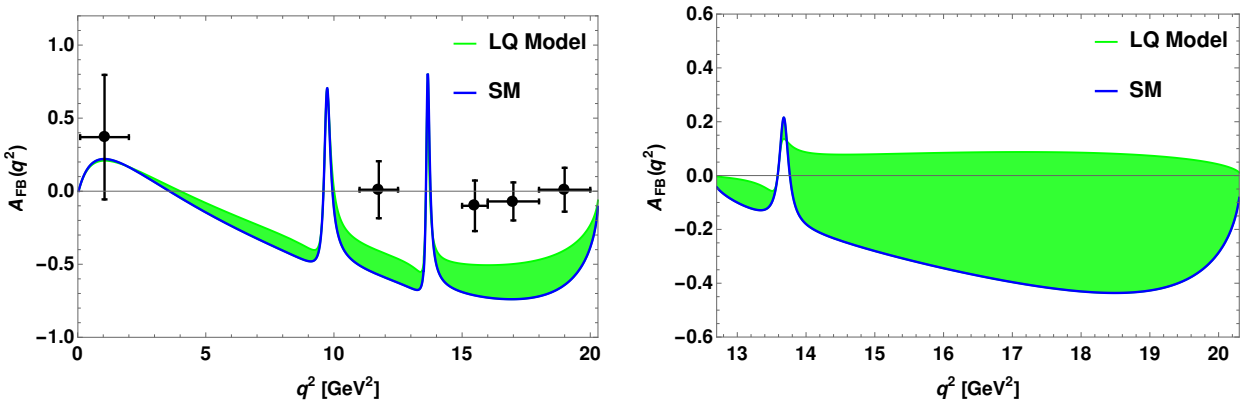

FIG. 4: Same as Fig.3 for $X = (3, 2, 1/6)$ LQ exchange.

are expected to have significantly large branching fractions. The observation of neutrino oscillation has provided unambiguous evidence for lepton flavour violation in the neutral lepton sector which in turn provides motivation to explore other LFV transitions such as $l_i \to l_j\gamma$, $l_i^- \to l_j^- l_k^+ l_k^-$, $B \to l_i^\pm l_j^\mp$ etc. Though there is no direct experimental evidence for such processes, but there exists experimental upper bounds on some of these modes. The LFV decays in the B meson and in the charged lepton sector have been widely investigated in the literature [29, 36, 50]. Therefore, it is interesting to see whether LFV decays could be observed in Λ_b decays also.

As discussed earlier, these processes occur at tree level due to the exchange of scalar leptoquarks. In the leptoquark model the effective Hamiltonian for $b \to s l_i^- l_j^+$ LFV process

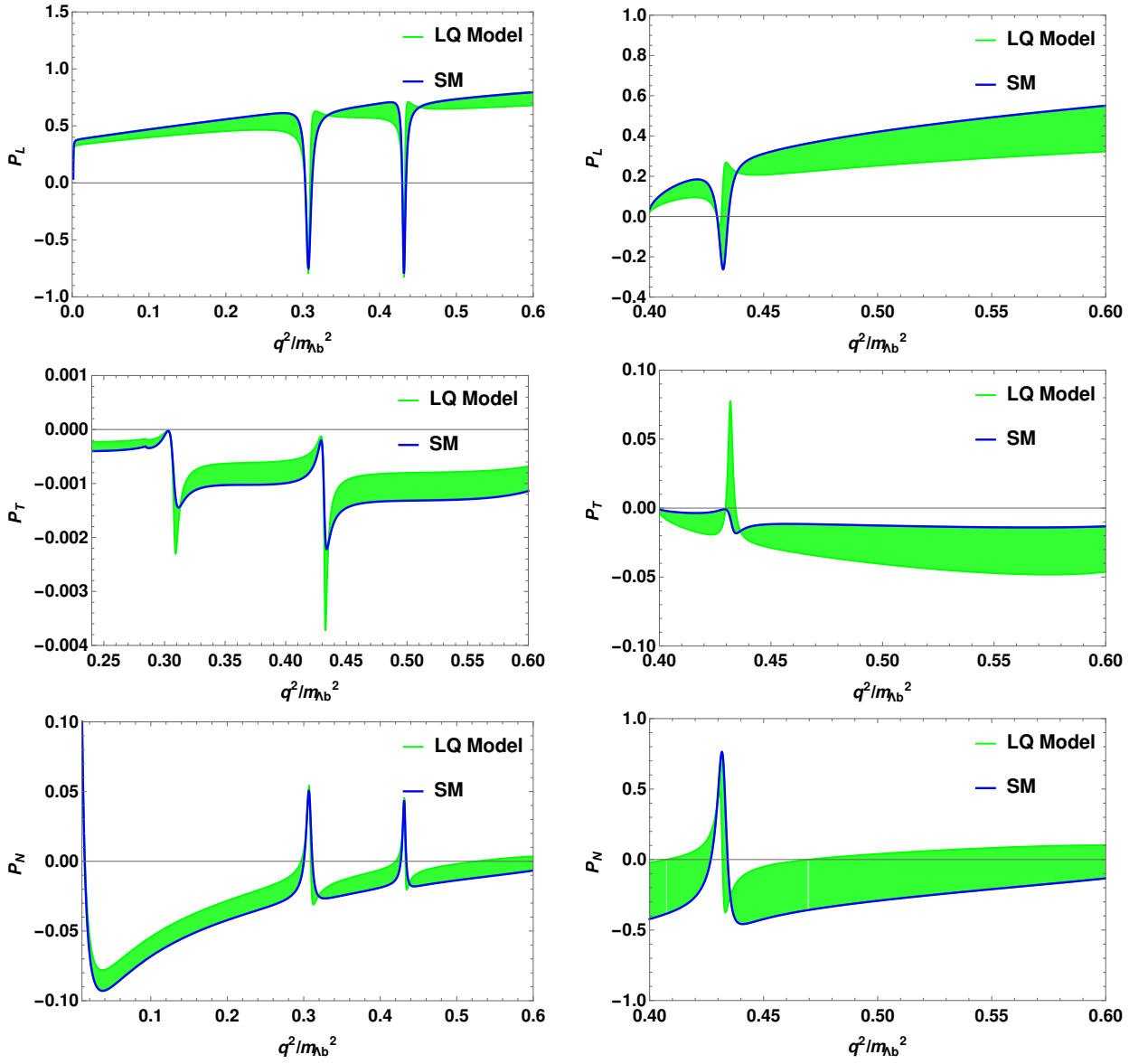

FIG. 5: The plots in the left panel represent the longitudinal (top), transverse (middle) and normal (bottom) polarizations for $\Lambda_b \to \Lambda\mu^+\mu^-$ precess with respect to $q^2/m^2_{\Lambda_b}$ in the $X = (3, 2, 7/6)$ LQ model. The corresponding plots for $\Lambda_b \to \Lambda\tau^+\tau^-$ mode are shown in the right panel.

is given as [29, 36]

$$\mathcal{H}_{LQ} = G_{LQ}\,(\bar{s}\gamma^\mu P_L b)\,(\bar{l}_i\gamma_\mu(1+\gamma_5)l_j), \tag{43}$$

where the coefficient G_{LQ} is

$$G_{LQ} = \frac{\lambda^{i3}\lambda^{j2*}}{8M_Y^2}\ . \tag{44}$$

Using the form factors given in the Appendix A, the amplitude for the LFV $\Lambda_b \to \Lambda l_i^- l_j^+$

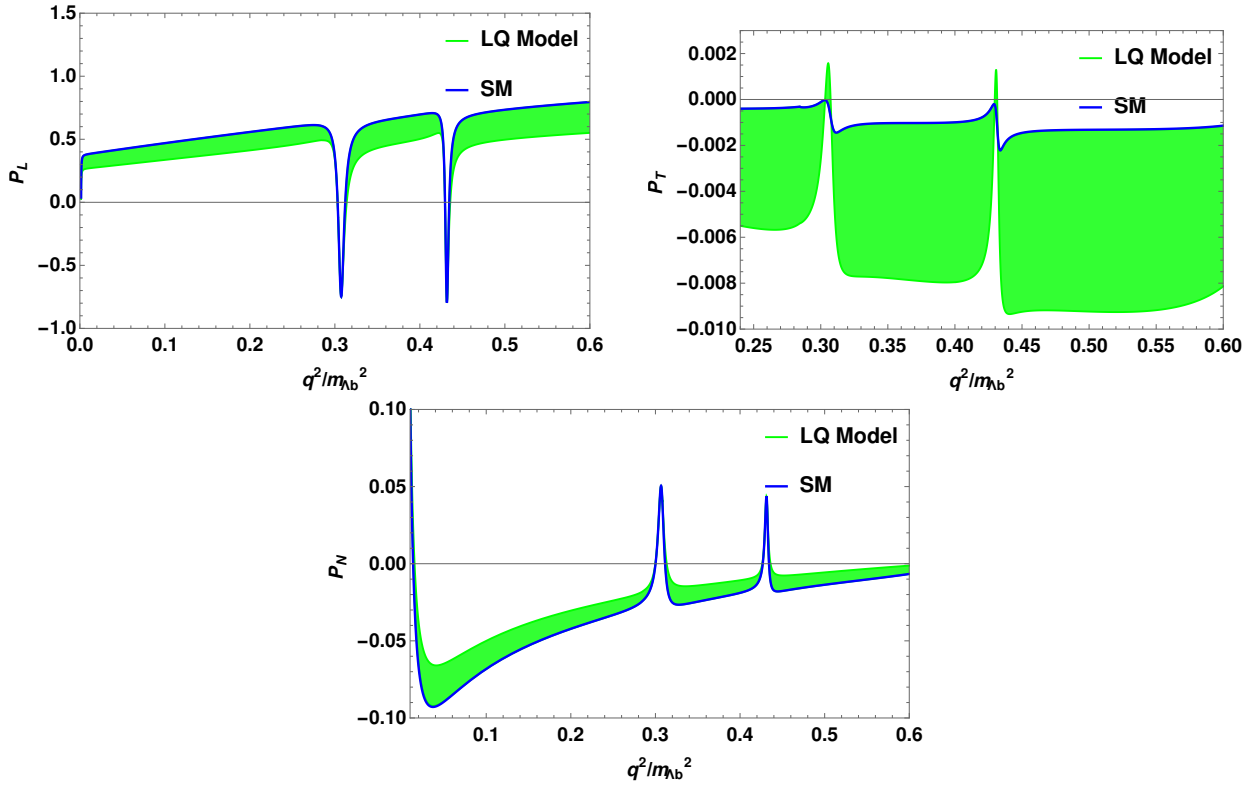

FIG. 6: The polarization plots of $\Lambda_b \to \Lambda\mu^+\mu^-$ process for $X = (3, 2, 1/6)$ LQ exchange.

decay is given by

$$\mathcal{M}(\Lambda_b \to \Lambda l_i^- l_j^+) = G_{LQ}\Bigg[\left(\bar{l}_i\gamma_\mu(1+\gamma_5)l_j\right)\Big\{\bar{u}_\Lambda\Big(\gamma^\mu(A_1'P_R + B_1'P_L)\Big)u_{\Lambda_b} + \bar{u}_\Lambda i\sigma_{\mu\nu}q^\nu(A_2'P_R + B_2'P_L)u_{\Lambda_b} + q^\mu\bar{u}_\Lambda(A_3'P_R + B_3'P_L)u_{\Lambda_b}\Big\}\Bigg]. \quad (45)$$

The coefficients A_k' and B_k' in (45) are related to the form factors through

$$A_k' = \frac{f_k - g_k}{2} \quad \text{and} \quad B_k' = \frac{f_k + g_k}{2}, \quad k = 1, 2, 3. \quad (46)$$

Now using this transition amplitude, the branching ratio for the $\Lambda_b \to \Lambda l_i^- l_j^+$ process is given as

$$\frac{d^2\Gamma}{d\hat{s}d\cos\theta} = \frac{|G_{LQ}|^2}{2^6\pi^3}m_{\Lambda_b}^5\frac{\sqrt{\lambda_1\lambda_2}}{\hat{s}}I(\hat{s}), \quad (47)$$

where

$$I(\hat{s}) = I_0(\hat{s}) + I_1(\hat{s})\cos\theta + I_2(\hat{s})\cos^2\theta, \quad (48)$$

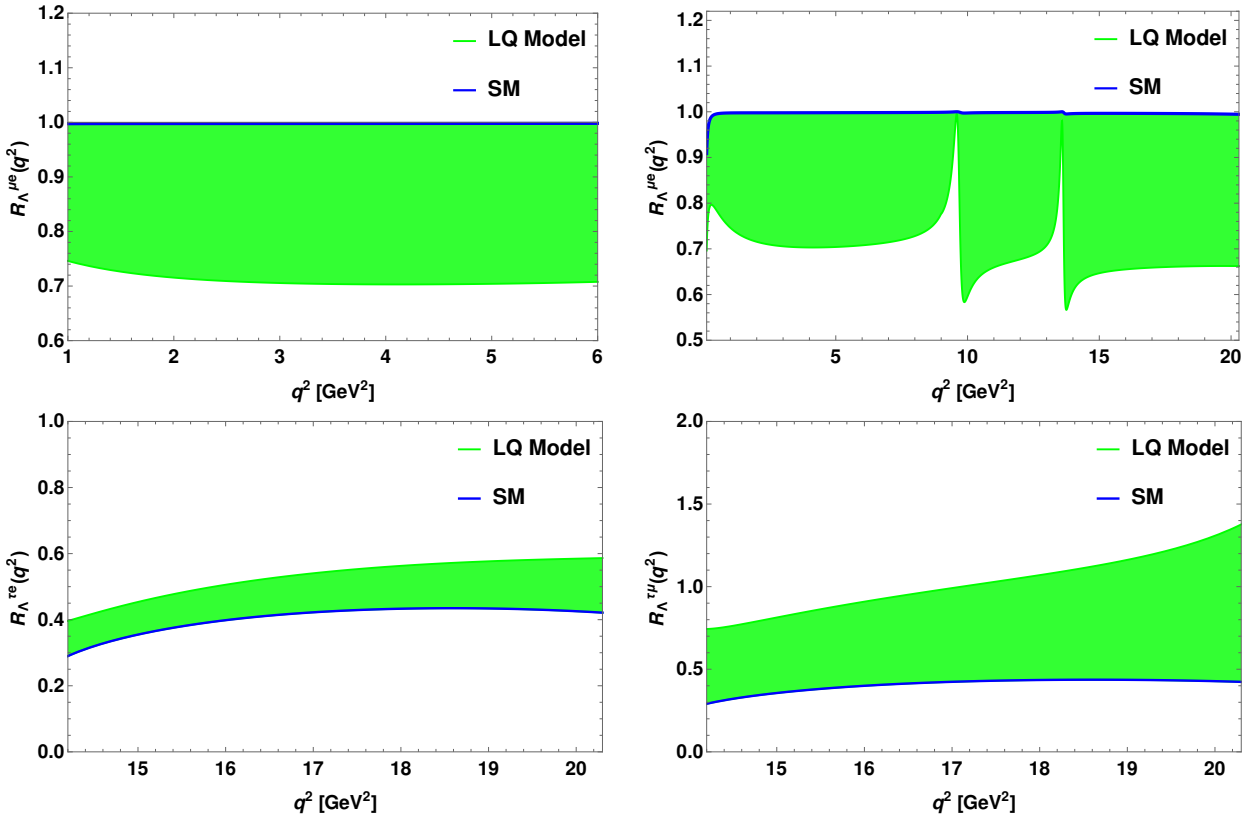

FIG. 7: The variation of lepton universality violation $R_\Lambda^{\mu e}$ (top-right panel), $R_\Lambda^{\tau e}$ (bottom-left panel) and $R_\Lambda^{\tau \mu}$ (bottom-right panel) with respect to q^2 for $X = (3, 2, 7/6)$ LQ exchange. Here $R_\Lambda^{\mu e}$ (top-left panel) shows the non-universality in the low $q^2 \in [1, 6]$ region.

with

$$
\begin{aligned}
I_0(\hat{s}) \;=\; & \frac{1}{4}\left(|A_1'|^2 + |B_1'|^2 + m_{\Lambda_b}^2 \hat{s}(|A_2'|^2 + |B_2'|^2)\right)\left[(1-r)^2 - \hat{s}^2\right] \\
& - \; 2\sqrt{r}\hat{s}\left(1 - \frac{m_i^2 + m_j^2}{q^2}\right)\left(Re(A_1' B_1'^*) + m_{\Lambda_b}^2 \hat{s} Re(A_2' B_2'^*)\right) \\
& - \; Re\left(A_2' B_2'^*\right)\sqrt{r}\left[-\frac{\left(m_i^2 - m_j^2\right)^2}{m_{\Lambda b}^2} + \hat{s}\left(m_i^2 + m_j^2\right)\right] \\
& + \; 2m_{\Lambda_b}\hat{s}\left(1 - \frac{(m_i^2 + m_j^2)}{2q^2}\right)\Big[\left(Re(A_1' A_2'^*) + Re(B_1' B_2'^*)\right)\sqrt{r}(1-t) \\
& - \; \Big(Re(A_1' B_2'^*) + Re(B_1' A_2'^*)\Big)(t-r)\Big] \\
& + \; \frac{(m_i^2 + m_j^2)}{m_{\Lambda_b}}\Big[\Big(Re(A_1' A_3'^*) + Re(B_1' B_3'^*)\Big)\sqrt{r}(1-t) + \Big(Re(A_1' B_3'^*) + Re(B_1' A_3'^*)\Big)(t-r)\Big] \\
& + \; \left[\hat{s}(m_i^2 + m_j^2) - \frac{(m_i^2 - m_j^2)^2}{m_{\Lambda_b}^2}\right]\left[\frac{t}{2}(|A_3'|^2 + |B_3'|^2) - \sqrt{r} Re(A_3' B_3'^*)\right], \qquad (49)
\end{aligned}
$$

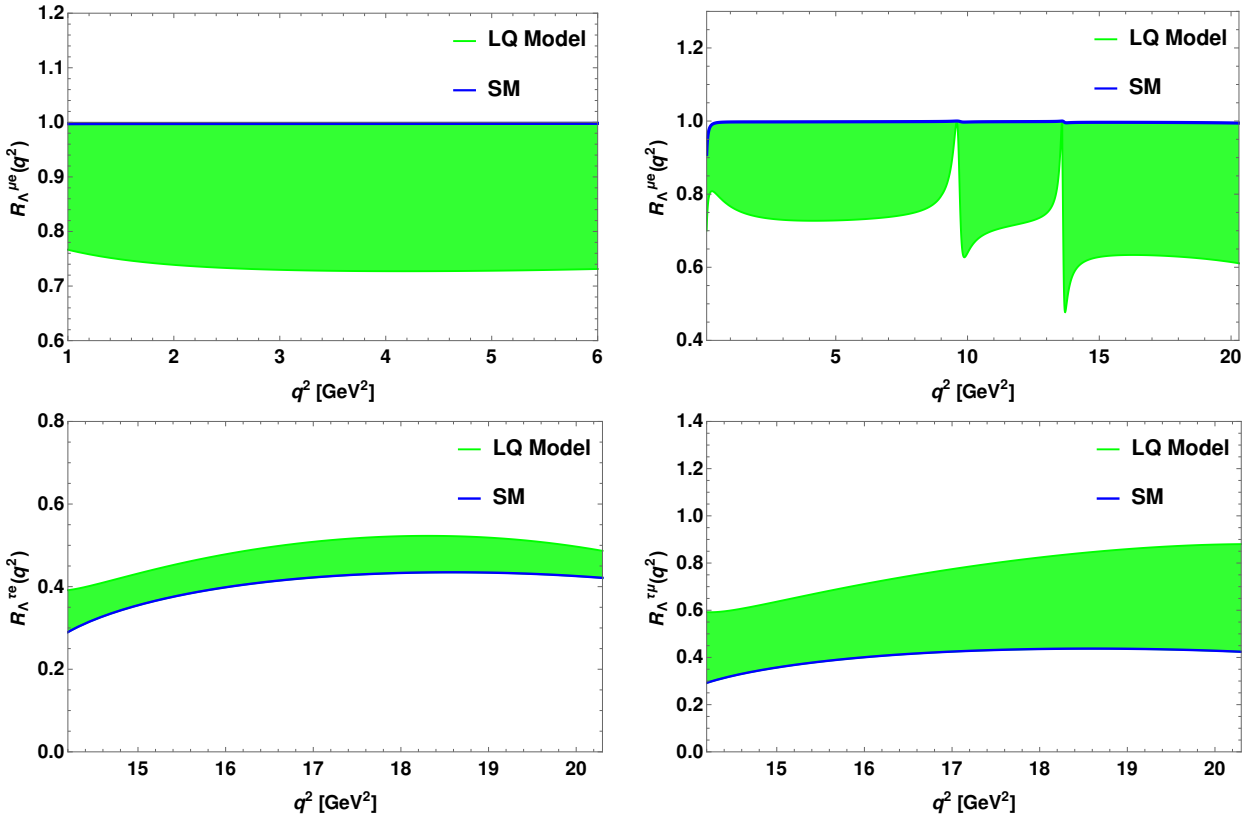

FIG. 8: Same as Fig.7 for $X = (3, 2, 1/6)$ LQ exchange.

$$
\begin{aligned}
I_1(\hat{s}) \;=\; & \frac{\sqrt{\lambda_1\lambda_2}}{\hat{s}}\Big[-\frac{1}{2}\hat{s}(|A_1'|^2-|B_1'|^2)+(m_j^2-m_i^2)(1-t-\frac{\hat{s}}{2})(|A_2'|^2+|B_2'|^2) \\
& + \frac{1}{2}\frac{m_j^2-m_i^2}{m_{\Lambda_b}}\left[\sqrt{r}\,(Re(A_1'A_2'^*)+Re(B_1'B_2'^*))-(Re(A_1'B_2'^*)+Re(B_1'A_2'^*))\right] \\
& + \frac{1}{2}\frac{m_j^2-m_i^2}{m_{\Lambda_b}}\left[\sqrt{r}\,(Re(A_1'A_3'^*)+Re(B_1'B_3'^*))+(Re(A_1'B_3'^*)+Re(B_1'A_3'^*))\right] \\
& + \frac{\hat{s}}{2}(m_i^2-m_j^2)\,(Re(A_2'A_3'^*)+Re(B_2'B_3'^*))\Big], \qquad (50)
\end{aligned}
$$

and

$$
I_2(\hat{s}) = \frac{\lambda_1\lambda_2}{\hat{s}^2}\left[-\frac{1}{4}\left(|A_1'|^2+|B_1'|^2-m_{\Lambda_b}^2\hat{s}(|A_2'|^2+|B_2'|^2)\right)\right]. \qquad (51)
$$

Here, $\lambda_1 = \lambda$ (as defined in section III), $\lambda_2 = \hat{m}_i^4+\hat{m}_j^4+\hat{s}^2-2\left(\hat{m}_i^2\hat{m}_j^2+\hat{m}_i^2\hat{s}+\hat{m}_j^2\hat{s}\right)$, and $t = (1+r-\hat{s})/2$. The full kinematically accessible physical range for these processes is given by

$$
(m_i+m_j)^2 \le q^2 \le (m_{\Lambda_b}-m_\Lambda)^2. \qquad (52)
$$

TABLE III: The predicted integrated values of the branching ratio, forward-backward asymmetry, lepton polarization asymmetry and the lepton non-universality with respect to their respective q^2 range for the $\Lambda_b \to \Lambda\mu(\tau)^+\mu(\tau)^-$ processes in the SM and the LQ model.

Observables	SM prediction	Values in $Y = 7/6$ LQ model	Values in $Y = 1/6$ LQ model
$\mathrm{Br}(\Lambda_b \to \Lambda e^+ e^-)$	$(1.168 \pm 0.134) \times 10^{-6}$	$(1.168 - 1.91) \times 10^{-6}$	$(1.168 - 2.13) \times 10^{-6}$
$\mathrm{Br}(\Lambda_b \to \Lambda \mu^+ \mu^-)$	$(1.165 \pm 0.132) \times 10^{-6}$	$(1.165 - 1.37) \times 10^{-6}$	$(1.165 - 1.52) \times 10^{-6}$
$\langle A_{FB}^{\mu} \rangle$	-0.567	$-0.567 \to -0.446$	$-0.567 \to -0.54$
$\langle P_L^{\mu} \rangle$	0.34	$0.3 - 0.34$	$0.24 - 0.34$
$\langle P_T^{\mu} \rangle$	-4.5×10^{-4}	$-(4.5 \to 2.87) \times 10^{-4}$	$-(0.45 \to 3.26) \times 10^{-3}$
$\langle P_N^{\mu} \rangle$	-0.0192	$-0.0192 \to -0.013$	$-0.0192 \to -0.012$
$\mathrm{Br}(\Lambda_b \to \Lambda \tau^+ \tau^-)$	$(2.13 \pm 0.215) \times 10^{-7}$	$(2.13 - 4.38) \times 10^{-7}$	$(2.13 - 8.32) \times 10^{-7}$
$\langle A_{FB}^{\tau} \rangle$	-0.38	$-0.38 \to 3.2 \times 10^{-3}$	$-0.38 \to 7.68 \times 10^{-2}$
$\langle P_L^{\tau} \rangle$	0.075	$0.047 - 0.075$	$6.3 \times 10^{-3} - 0.075$
$\langle P_T^{\tau} \rangle$	-2.3×10^{-3}	$-(7 \to 2.3) \times 10^{-3}$	$(-0.23 \to 2.0) \times 10^{-2}$
$\langle P_N^{\tau} \rangle$	-0.05	$-0.05 \to 8.1 \times 10^{-3}$	$-0.05 \to 0.0316$
$\langle R_{\Lambda_b}^{\mu e} \rangle$	0.997	$0.67 - 0.997$	$0.68 - 0.997$
$\langle R_{\Lambda_b}^{\mu e} \rangle_{[q^2 \in (1,6)]}$	0.998	$0.71 - 0.998$	$0.74 - 0.998$

As there is no intermediate particle in the SM which can decay into two leptons of different flavours, so in comparison with the $\Lambda_b \to \Lambda l^+ l^-$ processes, LFV decays have no long distance QCD contributions and dominant charmonium resonance background. The required input values for numerical evaluation are taken from [8] and the values of the q^2 dependent form factors are taken from LCSR approach [21]. To determine the values of various LQ couplings, which are involved in the LFV decays, we use the following assumptions. As we know that the expansion parameter of the CKM matrix in the Wolfenstein parametrization (λ), can be related to the down type quark masses as $\lambda \sim (m_d/m_s)^{1/2}$ in the quark sector, while in the lepton sector one can have the same order for λ with the relation $\lambda \sim (m_{l_i}/m_{l_j})^{1/4}$. Hence, for other required leptoquark coupling, we assume that the coupling between different generation of quarks and leptons follow the simple scaling laws, i.e., $\lambda^{ij} = (m_i/m_j)^{1/4}\lambda^{ii}$

with $j > i$. Thus, using the values of the leptoquark coupling as given in Table I, one can obtain the bound on required LQ couplings involved in LFV decays. Using these values we plot the variation of branching ratio of LFV decays such as $\Lambda_b \to \Lambda\mu^- e^+$ (top left panel), $\Lambda_b \to \Lambda\tau^- e^+$ (top right panel) and $\Lambda_b \to \Lambda\tau^- \mu^+$ (lower panel) with respect to q^2 in Fig. 9 and the predicted upper limits of the branching ratios are given in Table IV. So far there is no experimental evidence on the LFV Λ_b decays. However, since the predicted branching ratios are $\mathcal{O}(10^{-9})$, they can be searched at LHCb and exploration/observation of these modes would definitely shed some light in the leptoquark scenarios.

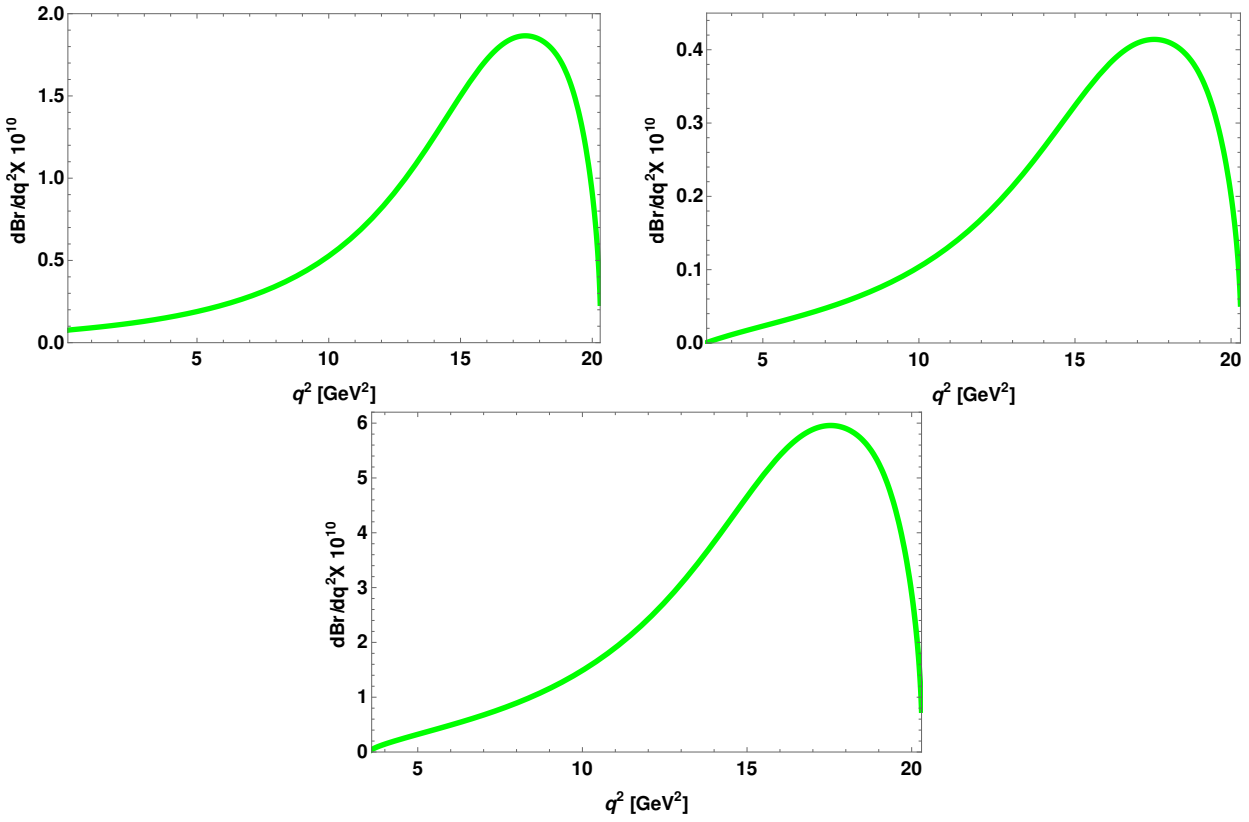

FIG. 9: The variation of branching ratio of LFV $\Lambda_b \to \Lambda\mu^- e^+$ (left panel), $\Lambda_b \to \Lambda\tau^- e^+$ (right panel) and $\Lambda_b \to \Lambda\tau^- \mu^+$ (bottom panel) processes with respect to q^2 in the $X = (3, 2, 7/6)$ leptoquark model. Here the required leptoquark couplings are computed by using the scaling ansatz $\lambda^{ij} = (m_i/m_j)^{1/4}\lambda^{ii}$.

TABLE IV: The predicted upper limits of the branching ratios, which are obtained using the upper limits of the LQ couplings, of LFV $\Lambda_b \to \Lambda l_i^- l_j^+$ processes, $l = e, \mu, \tau$ in the $X = (3, 2, 7/6)$ leptoquark model. Also the required leptoquark couplings are computed by using the scaling ansatz $\lambda^{ij} = (m_i/m_j)^{1/4}\lambda^{ii}$.

Decay process	Predicted branching ratio
$\Lambda_b \to \Lambda\mu^- e^+$	1.56×10^{-9}
$\Lambda_b \to \Lambda\tau^- e^+$	3.2×10^{-10}
$\Lambda_b \to \Lambda\tau^- \mu^+$	4.6×10^{-9}

VI. CONCLUSION

In this paper, we have studied the rare semileptonic $\Lambda_b \to \Lambda l^+ l^-$, $l = e, \mu, \tau$ baryonic decays in the scalar leptoquark model. The leptoquark parameter space has been constrained using the experimental limits on the branching ratios of the two body leptonic decays $B_s \to l^+ l^-$. We have computed the branching ratios, the forward-backward and lepton polarization asymmetries ($P_{L,T,N}$) using the new leptoquark couplings. We have shown explicitly the results for both the relevant $X = (3, 2, 7/6)$ and $X = (3, 2, 1/6)$ leptoquark models. The zero-position of the forward-backward asymmetry is found to be insensitive to the additional leptoquark effect. These models also give negligible contribution to the transverse polarization asymmetry. In addition, we also estimated the lepton universality violation parameters in these decays analogous to R_K in $B \to K l^+ l^-$ process. The lepton flavour violating Λ_b decays are also studied and the predicted upper limits on these branching ratios are found to be $\mathcal{O}(10^{-10} - 10^{-9})$, which could be searched in the LHCb experiment.

Appendix A: Form Factors in $\Lambda_b \to \Lambda$ transition

The transition form factors for $\Lambda_b(P) \to \Lambda(p')$ decays can be parameterized as [16, 43]

$$\begin{aligned}
\langle \Lambda(p')|\bar{s}\gamma_\mu b|\Lambda_b(P)\rangle &= f_1 \bar{u}_\Lambda \gamma_\mu u_{\Lambda_b} + f_2 \bar{u}_\Lambda i\sigma_{\mu\nu}q^\nu u_{\Lambda_b} + f_3 q_\mu \bar{u}_\Lambda u_{\Lambda_b},\\
\langle \Lambda(p')|\bar{s}\gamma_\mu\gamma_5 b|\Lambda_b(P)\rangle &= g_1 \bar{u}_\Lambda \gamma_\mu\gamma_5 u_{\Lambda_b} + g_2 \bar{u}_\Lambda i\sigma_{\mu\nu}q^\nu\gamma_5 u_{\Lambda_b} + g_3 q_\mu \bar{u}_\Lambda\gamma_5 u_{\Lambda_b},\\
\langle \Lambda(p')|\bar{s}i\sigma_{\mu\nu} b|\Lambda_b(P)\rangle &= f_T \bar{u}_\Lambda i\sigma_{\mu\nu} u_{\Lambda_b} + f_T^V \bar{u}_\Lambda \left(\gamma_\mu q_\nu - \gamma_\nu q_\mu\right) u_{\Lambda_b} + f_T^S \left(P_\mu q_\nu - P_\nu q_\mu\right)\bar{u}_\Lambda u_{\Lambda_b},\\
\langle \Lambda(p')|\bar{s}i\sigma_{\mu\nu}\gamma_5 b|\Lambda_b(P)\rangle &= g_T \bar{u}_\Lambda i\sigma_{\mu\nu}\gamma_5 u_{\Lambda_b} + g_T^V \bar{u}_\Lambda \left(\gamma_\mu q_\nu - \gamma_\nu q_\mu\right)\gamma_5 u_{\Lambda_b}\\
&\quad + g_T^S \left(P_\mu q_\nu - P_\nu q_\mu\right)\bar{u}_\Lambda\gamma_5 u_{\Lambda_b},
\end{aligned} \tag{A1}$$

and for dipole operators

$$\langle \Lambda(p')|\, \bar{s}i\sigma_{\mu\nu}q^\nu b\,|\Lambda_b(P)\rangle = f_1^T \bar{u}_\Lambda\gamma_\mu u_{\Lambda_b} + f_2^T \bar{u}_\Lambda i\sigma_{\mu\nu}q^\nu u_{\Lambda_b} + f_3^T q_\mu \bar{u}_\Lambda u_{\Lambda_b}, \tag{A2}$$

$$\langle \Lambda(p')|\, \bar{s}i\sigma_{\mu\nu}q^\nu\gamma_5 b\,|\Lambda_b(P)\rangle = g_1^T \bar{u}_\Lambda\gamma_\mu\gamma_5 u_{\Lambda_b} + g_2^T \bar{u}_\Lambda i\sigma_{\mu\nu}q^\nu\gamma_5 u_{\Lambda_b} + g_3^T q_\mu \bar{u}_\Lambda\gamma_5 u_{\Lambda_b}. \tag{A3}$$

with $q = P - p'$ and

$$\begin{aligned}
f_2^T &= f_T - f_T^S q^2\,,\\
f_1^T &= \left[f_T^V + f_T^S\left(M_\Lambda + M_{\Lambda_b}\right)\right] q^2\,,\\
f_1^T &= -\frac{q^2}{\left(M_{\Lambda_b} - M_\Lambda\right)} f_3^T\,,\\
g_2^T &= g_T - g_T^S q^2\,,\\
g_1^T &= \left[g_T^V + g_T^S\left(M_\Lambda - M_{\Lambda_b}\right)\right] q^2\,,\\
g_1^T &= \frac{q^2}{\left(M_{\Lambda_b} + M_\Lambda\right)} g_3^T\,.
\end{aligned} \tag{A4}$$

Appendix B: Expressions for $\mathcal{K}_{0,1,2}(\hat{s})$ functions

The complete expressions for $\mathcal{K}_{0,1,2}(\hat{s})$ functions required to calculate the double differential decay rate is given by [18]

$$
\begin{aligned}
\mathcal{K}_0(\hat{s}) &= 32m_l^2 m_{\Lambda_b}^2 \hat{s}(1+r-\hat{s})(|D_3|^2+|E_3|^2) \\
&+ 64m_l^2 m_{\Lambda_b}^3 (1-r-\hat{s}) Re(D_1^* E_3 + D_3 E_1^*) + 64m_{\Lambda_b}^2 \sqrt{r}(6m_l^2 - \hat{s}m_{\Lambda_b}^2) Re(D_1^* E_1) \\
&+ 64m_l^2 m_{\Lambda_b}^3 \sqrt{r}\Big(2m_{\Lambda_b}\hat{s} Re(D_3^* E_3) + (1-r+\hat{s}) Re(D_1^* D_3 + E_1^* E_3)\Big) \\
&+ 32m_{\Lambda_b}^2 (2m_l^2 + m_{\Lambda_b}^2 \hat{s})\Big((1-r+\hat{s}) m_{\Lambda_b}\sqrt{r} Re(A_1^* A_2 + B_1^* B_2) \\
&- m_{\Lambda_b}(1-r-\hat{s}) Re(A_1^* B_2 + A_2^* B_1) - 2\sqrt{r}\Big[Re(A_1^* B_1) + m_{\Lambda_b}^2 \hat{s} Re(A_2^* B_2)\Big]\Big) \\
&+ 8m_{\Lambda_b}^2 \Big(4m_l^2(1+r-\hat{s}) + m_{\Lambda_b}^2[(1-r)^2 - \hat{s}^2]\Big)\Big(|A_1|^2 + |B_1|^2\Big) \\
&+ 8m_{\Lambda_b}^4 \Big(4m_l^2[\lambda + (1+r-\hat{s})\hat{s}] + m_{\Lambda_b}^2 \hat{s}[(1-r)^2 - \hat{s}^2]\Big)\Big(|A_2|^2 + |B_2|^2\Big) \\
&- 8m_{\Lambda_b}^2 \Big(4m_l^2(1+r-\hat{s}) - m_{\Lambda_b}^2[(1-r)^2 - \hat{s}^2]\Big)\Big(|D_1|^2 + |E_1|^2\Big) \\
&+ 8m_{\Lambda_b}^5 \hat{s} v_l^2 \Big(- 8m_{\Lambda_b}\hat{s}\sqrt{r} Re(D_2^* E_2) + 4(1-r+\hat{s})\sqrt{r} Re(D_1^* D_2 + E_1^* E_2) \\
&- 4(1-r-\hat{s}) Re(D_1^* E_2 + D_2^* E_1) + m_{\Lambda_b}[(1-r)^2 - \hat{s}^2]\Big[|D_2|^2 + |E_2|^2\Big]\Big) \,, \qquad \text{(B1)}
\end{aligned}
$$

$$
\begin{aligned}
\mathcal{K}_1(\hat{s}) &= -16m_{\Lambda_b}^4 \hat{s} v_l \sqrt{\lambda}\Big\{2Re(A_1^* D_1) - 2Re(B_1^* E_1) \\
&+ 2m_{\Lambda_b} Re(B_1^* D_2 - B_2^* D_1 + A_2^* E_1 - A_1^* E_2)\Big\} \\
&+ 32m_{\Lambda_b}^5 \hat{s}\; v_l \sqrt{\lambda}\Big\{m_{\Lambda_b}(1-r) Re(A_2^* D_2 - B_2^* E_2) \\
&+ \sqrt{r} Re(A_2^* D_1 + A_1^* D_2 - B_2^* E_1 - B_1^* E_2)\Big\} \,, \qquad \text{(B2)}
\end{aligned}
$$

and

$$
\begin{aligned}
\mathcal{K}_2(\hat{s}) &= 8m_{\Lambda_b}^6 v_l^2\; \lambda\hat{s}\; \Big((|A_2|^2 + |B_2|^2 + |D_2|^2 + |E_2|^2\Big) \\
&- 8m_{\Lambda_b}^4 v_l^2\; \lambda\; \Big(|A_1|^2 + |B_1|^2 + |D_1|^2 + |E_1|^2\Big) \,. \qquad \text{(B3)}
\end{aligned}
$$

Acknowledgments

We would like to thank Science and Engineering Research Board (SERB) for financial support through grant No. SB/S2/HEP-017/2013.

[1] R. Aaij et al., [LHCb Collaboration], Phys. Rev. Lett. **111**, 191801 (2013), [arXiv:1308.1707 [hep-ex]].

[2] R. Aaij et al., [LHCb Collaboration], JHEP **02** (2016) 104, [arXiv:1512.04442].

[3] A. Abdesselam *et al.* [Belle Collaboration], arXiv:1604.04042 [hep-ex].

[4] R. Aaij et al., [LHCb Collaboration], Phys. Rev. Lett. **113**, 151601 (2014) [arXiv:1406.6482].

[5] R. Aaij et al., [LHCb Collaboration], JHEP **1406**, 133 (2014) [arXiv:1403.8044].

[6] R. Aaij et al., [LHCb Collaboration], Phys. Rev. Lett. **111**, 191801 (2013) [arXiv:1308.1707].

[7] R. Aaij et al., [LHCb Collaboration], JHEP **1307**, 084 (2013) [arXiv:1305.2168].

[8] K.A. Olive et al. (Particle Data Group), Chin. Phys. C, 38, 090001 (2014).

[9] S. Descotes-Genon, J. Matias, M. Ramon, J. Virto, JHEP **1301**, 048 (2013) [arXiv:1207.2753].

[10] S. Jager, J. Martin Camalich, JHEP **05**, 043 (2013) [arXiv:1212.2263]; S. Descotes-Genon, L. Hofer, J. Matias and J. Virto, JHEP **1412**, 125 (2014) [arXiv:1407.8526].

[11] S. Descotes-Genon, L. Hofer, J. Matias, J. Virto, JHEP **06**, 092 (2016) [arXiv:1510.04239].

[12] T. Huber, T. Hurth and E. Lunghi, Nucl. Phys. B **802**, 40 (2008),[arXiv:0712.3009].

[13] F. Beaujean, C. Bobeth, and D. van Dyk, Eur. Phys. J. C **74**, 2897, (2014) [arXiv:1310.2478]; T. Hurth and F. Mahmoudi, JHEP **04**, 097 (2014) [arXiv:1312.5267]; W. Altmannshofer, S. Gori, M. Pospelov and I. Yavin, Phys. Rev. D **89**, 095033 (2014) [arXiv: 1403.1269]; G. Hiller and M. Schmaltz, Phys. Rev. D **90**, 054014 (2014) [arXiv:1408.1627]; D. Aristizabal sierra, F. Staub and A. Vicente, Phys. Rev. D **92**, 015001 (2015) [arXiv:1503.06077]; Sofiane M. Boucenna, Jose W. F. Valle and A. Vicente, [arXiv:1503.07099]; F. Mahmoudi, S. Neshatpour, J. Virto, Eur. Phys. J. C **74** (2014) 2927, [arXiv:1401.2145]; A. Crivellin, G. D'Ambrasio, J. Heeck, Phys. Rev. Lett. **114**, 151801 (2015) [arXiv:1501.00993]; A. Crivellin, G. D'Ambrasio, J. Heeck, Phys. Rev. D **91**, 075006 (2015) [arXiv:1503.03477]; A. Crivellin, L. Hofer, J. Matias, U. Nierste, S. Pokorski, J. Rosiek, Phys. Rev. D **92**, 054013 (2015) [arXiv:1504.07928]; D. Becirevic, S. Fajfer, N. Kosnik, Phys. Rev. D **92**, 014016 (2015) [arXiv:1503.09024]; R. Alonso, B. Grinstein and J. Martin Camalich, Phys. Rev. Lett. **113**, 241802 (2014) [arXiv:1407.7044]; B. Gripaios, M. Nardecchia, S. A. Renner, JHEP **1505** (2015) 006, [arXiv:1412.1791]; A. Falkowski, M. Nardecchia, Robert Ziegler, [arXiv:1509.01249]; L. Calibbi, A. Crivellin, T. Ota, [arXiv:1506.02661]; S. Descotes-Genon, J. Matias and J. Virto, Phys. Rev. D **88**, 074002 (2013), [arXiv:1307.5683 [hep-ph]].

[14] S. Meinel, D. van Dyk, [arXiv:1603.02974].

[15] R. Aaij et al., [LHCb Collaboration], JHEP **06**, 115 (2015) [arXiv:1503.07138].

[16] Chaun-Hung Chen and C.Q. Geng, Phys. Rev. D **63**, 054005 (2001); Phys. Rev. D **63**, 114024 (2001); Phys. Rev D **64**, 074001 (2001).

[17] V. Bashity and K. Azizi, JHEP **0707**, 064 (2007) [arXiv:hep-ph/0702044].

[18] A. K. Giri and R. Mohanta, Eur. Phys. J. C**45**, 151-158 (2006), [arXiv:hep-ph/0510171]; Jour. Phys. G **31**, 1559 (2005); R. Mohanta and A. K. Giri, Phys. Rev. D **82**, 094022 (2010) [arXiv:1010.1152]

[19] Chaun-Hung Chen and C.Q. Geng, Phys. Lett. B **516**, 327 (2001) [arXiv:hep-ph/0101201]; C. S. Huang and H. J. Han, Phys. Rev. D **59**, 114022 (1999); Erratum *ibid*, **61**, 039901 (2000).

[20] W. Detmold, S. Meinel, Phys. Rev. D **93**, 074501 (2016) [arXiv:1602.01399]; G. Kumar and N. Mahajan, [arXiv:1511.00935]; W. Detmold, C-J David Lin, S. Meinel and M. Wingate, Phys. Rev. D **87**, 074502 (2013); K. Azizi and N. Katirci Eur. Phys. J. A **48**, 73 (2012); T. M. Aliev, A. Ozpineci, M. Savci, Nucl. Phys. B **649**, 168-188 (2003), [arXiv:hep-ph/0202120]; T. M. Aliev, A. Ozpineci and M. Savci, Phys. Rev. D **65**, 115002 (2002); *ibid* **D 67**, 035007 (2003); Nucl. Phys. B **709**, 115 (2005); T. M. Aliev, A. Ozpineci, M. Savci and C. Yüce, Phys. Lett. B **542**, 249 (2002); T. Gutsche, M. A. Ivanov, J. G. Korner, V. E. Lyubovitskij, P. Santorelli, Phys.Rev.D **87**, 074031 (2013), [arXiv:1301.3737]; P. Boer, T. Feldmann and D. van Dyk, JHEP **1501**, 155 (2015), [arXiv:1410.2115 [hep-ph]]; T. Feldmann and M. W. Y. Yip, Phys. Rev. D **85**, 014035 (2012), Erratum: [Phys. Rev. D **86**, 079901 (2012)], [arXiv:1111.1844 [hep-ph]].

[21] Yu-ming Wang, Ying Li and Cai-Dian Lu, Eur. Phys. J.C **59**, 861 (2009), [arXiv:0804.0648].

[22] W. Detmold, C. J. David Lin, S. Meinel, and M. Wingate, [arXiv: 1212.4827[hep-lat]].

[23] W. Detmold, S. Meinel, Phys. Rev. D **93**, 074501 (2016), [arXiv: 1602.01399[hep-lat]].

[24] H. Georgi and S. L. Glashow, Phys. Rev. Lett. **32**, 438 (1974).

[25] H. Georgi, AIP Conf. Proc. **23** 575 (1975); H. Fritzsch and P. Minkowski, Annals Phys. **93**, 193 (1975); P. Langacker, Phys. Rep. **72**, 185 (1981).

[26] J. C. Pati and A. Salam, Phys. Rev. D **10**, 275 (1974).

[27] B. Schrempp and F. Shrempp, Phys. Lett.B **153**, 101 (1985); B. Gripaios, JHEP **1002**, 045 (2010) [arXiv:0910.1789].

[28] D. B. Kaplan, Nucl. Phys. B **365**, 259 (1991).

[29] S. Sahoo and R. Mohanta, Phys. Rev. D **91**, 094019 (2015) [arXiv:1501.05193].

[30] R. Mohanta, Phys. Rev. D **89**, 014020 (2014) [arXiv:1310.0713].

[31] S. Sahoo and R. Mohanta, Phys.Rev. D **93**, 034018 (2016) [arXiv:1507.02070].

[32] S. Davidson, D. C. Bailey and B. A. Campbell, Z. Phys. C **61**, 613 (1994), hep-ph/9309310; I.

Dorsner, S. Fajfer, J. F. Kamenik, N. Kosnik, Phys. Lett. B **682**, 67 (2009); [arXiv:0906.5585]; S. Fajfer, N. Kosnik, Phys. Rev. D **79**, 017502 (2009), [arXiv:0810.4858]; R. Benbrik, M. Chabab, G. Faisel,[arXiv:1009.3886] ; A. V. Povarov, A. D. Smirnov, [arXiv:1010.5707]; J. P Saha, B. Misra and A. Kundu, Phys. Rev.D **81**, 095011 (2010) [arXiv:1003.1384]; I. Dorsner, J. Drobnak, S. Fajfer, J. F. Kamenik, N. Kosnik, JHEP **11**, 002 (2011) [arXiv: 1107.5393]; F. S. Queiroz, K. Sinha, A. Strumia, [arXiv:1409.6301]; B. Allanach,A. Alves, F. S. Queiroz, K. Sinha, A. Strumia, [arXiv:1501.03494]; Ivo de M. Varzielas, G. Hiller, JHEP 1506 (2005) 072, [arXiv:1503.01084]; S. Sahoo and R. Mohanta, New Jour. Phys. **18**, 013032 (2016) [arXiv:1509.06248]; M. Bauer and M. Neubert, [arXiv:1511.01900]; S. Fajfer and N. Kosnik, [arXiv:1511.06024].

[33] J. M. Arnold, B. Fornal and M. B. Wise, Phys. Rev. D **88**, 035009 (2013), [arXiv:1304.6119].

[34] N. Kosnik, Phys. Rev. D **86**, 055004 (2012), [arXiv:1206.2970].

[35] D. Aristizabal Sierra, M. Hirsch, S. G. Kovalenko, Phys. Rev. D **77**, 055011 (2008), [arXiv:0710.5699]; K.S. Babu, J. Julio, Nucl. Phys. B **841**, 130 (2010), [arXiv:1006.1092]; S. Davidson, S. Descotes-Genon, JHEP **1011**, 073 (2010), [arXiv:1009.1998]; S. Fajfer, J. F. Kamenik, I. Nisandzic, J. Zupan, Phys. Rev. Lett. **109**, 161801, (2012), [arXiv:1206.1872]; K. Cheung, W.-Y. Keung, P.-Y. Tseng, [arXiv:1508.01897]; D. A. Camargo, [arXiv:1509.04263]; S. Baek, K. Nishiwaki, [arXiv:1509.07410]; Heinrich Pas, Erik Schumacher, Phys. Rev. D **92**, 114025 (2015) [arXiv:1510.08757]; S. M. Boucenna, A. Celis, J. Fuentes-Martin, A. Vicente and J. Virto, Phys. Lett. B **760**, 214 (2016), [arXiv:1604.03088 [hep-ph]].

[36] S. Sahoo and R. Mohanta, Phys. Rev. D **93**, 114001 (2016) [arXiv:1512.04657].

[37] Shuai-wei Wang, Ya-dong Yang, [arXiv: 1608.03662[hep-ph]].

[38] G. Buchalla, A.J. Buras, M. Lautenbacher, Rev. Mod. Phys. **68**, 1125 (1996).

[39] W. Altmannshofer, P. Ball, A. Bharucha, A. J. Buras, D. M. Straub and M. Wick, JHEP **0901**, 019 (2009), [arXiv:0811.1214].

[40] A. J. Buras and M. Munz, Phys. Rev. D **52** (1995) 186; M. Misiak, Nucl. Phys. B 393 (1993) 23; Erratum, *ibid.* B **439**, 461 (1995).

[41] C. S. Lim, T. Morozumi and A. I. Sanda, Phys. Lett. B. **218**, 343 (1989); N. G. Deshpande, J. Trampetic and K. Ponose, Phys. Rev. D **39**, 1461 (1989); P. J. O'Donnell and H. K.K. Tung, Phys. Rev. D **43**, 2067 (1991); P. J. O'Donnell, M. Sutherland and H. K.K. Tung, Phys. Rev. D **46**, 4091 (1992); F. Krüger and L. M. Sehgal, Phys. Lett. B **380**, 199 (1996).

[42] A. Ali, P. Ball, L. T. Handoko, and G. Hiller, Phys. Rev. D**61**, 074024 (2000).

[43] T. Mannel, W. Roberts and Z. Ryzak, Nucl. Phys. B **355**, 38 (1991); T. Mannel and S. Recksiegel J. Phys. **G24**, 979 (1998).

[44] C. Bobeth, M. Gorbahn, T. Hermann, M. Misiak, E. Stamou, M. Steinhauser, Phys. Rev.Lett. **112**, 101801 (2014) [arXiv:1311.0903].

[45] S. Chatrchyan et al., [CMS Collaboration], Phys. Rev. Lett. **111**, 101805 (2013), [arXiv:1307.5025].

[46] R. Aaij et al., [LHCb Collaboration], Phys. Rev. Lett. **111**, 101805 (2013), [arXiv:1307.5024].

[47] V. Khachatryan et al. [CMS Collaboration] and I. Bediaga et al. [LHCb Collaboration], Nature (London) **522**, 68 (2015).

[48] T. Inami and C. S. Lim, Prog. Theor. Phys. **65**, 297 (1981); [Erratum-ibid. **65**, 1772 (1981)].

[49] J. Charles *et al.*, Phys. Rev. D **91**, 073007 (2015), [arXiv:1501.05013].

[50] I. Ilakovac and A. Pilaftsis, Nucl. Phys. B **437**, 491 (1995) [hep-ph/9403398]; R. Barbieri, L. H. Hall and A. Strumia, Nucl. Phys. B **445**, 219 (1995) [hep-ph/9501334]; J. Hisano, T. Moroi, K. Tobe and M. Yamaguchi, Phys. Rev. D. **53**, 2442 (1996) [hep-ph/9510309]; J. R. Ellis, J. Hisano, M. Raidal and Y. Shimizu, Phys. Rev. D **66**, 115013 (2002) [hep-ph/0206110]; A. Brignole and A. Rossi, Nucl. Phys. B **701**, 3 (2004) [hep-ph/0404211]; A. Masiero, S. Profumo, S. Vempati and C. E. Yaguna, JHEP **0403** 046 (2004) [hep-ph/0401138]; A. Arganda and M. J. Herrero, Phys. Rev. D **73**, 055003 (2006) [hep-ph/0510405]; A. Antusch, E. Erganda, M. J. Herrero and A. M. Teixeira, JHEP **0611** 090 (2006) [hep-ph/0607263]; P. Paradisi, JHEP **0510**, 006 (2005) [hep-ph/0505046]; JHEP **0602** 050 (2006) [hep-ph/0508054]; JHEP **0608**, 047 (2006) [hep-ph/0611100]; A. G. Akeroyd, M. Aoki and Y. Okada, Phys. Rev. D **76**, 013004 (2007) [hep-ph/0610344]; B. M. Dassinger, T. Feldmann, T. Mannel, S. Turczyk, JHEP **0710**, 039 (2007) [arXiv:0707.0988]; R. Mohanta, Euro Phys. J. C **71**, 1625 (2011) [arXiv:1011.4184]; R. Alonso, B. Grinstein and J. M. Camalich, [arXiv: 1505.05164]; Chao-Jung Lee and J. Tandean, JHEP **08**, 123 (2015), [arXiv: 1505.04692]; W. Altmannshofer and I. Yavin, Phys Rev D. **92**, 075022 (2015) [arXiv:1508.07009].